

**Biz1, a zinc finger protein that is required for plant invasion by  
*Ustilago maydis* regulates the levels of a mitotic cyclin**

**Ignacio Flor-Parra<sup>a1</sup>, Miroslav Vranes<sup>b1</sup>, Jörg Kämper<sup>b</sup> and José Pérez-  
Martín<sup>a2</sup>**

<sup>a</sup>Departamento de Biotecnología Microbiana, Centro Nacional de Biotecnología  
CSIC, Campus de Cantoblanco-UAM, 28049 Madrid, Spain

<sup>b</sup>Max-Planck-Institut für Terrestrische Mikrobiologie, Abteilung Organismische  
Interaktionen, Karl-von-Frisch-Strasse, D-35043 Marburg, Germany

1 These authors contributed equally to this work

2 To whom correspondence should be addressed:

The author responsible for distribution of materials integral to the findings presented in this article in accordance with the policy described in the Instructions for Authors ([www.plantcell.org](http://www.plantcell.org)) is Dr. José Pérez-Martín, Departamento de Biotecnología Microbiana, Centro Nacional de Biotecnología-CSIC, Campus de Cantoblanco-UAM, 28049 Madrid, Spain. Phone: +34-91-585-4704; FAX: +34-91-585-4506; e-mail: [jperez@cnb.uam.es](mailto:jperez@cnb.uam.es)

**Key Words:** *Ustilago maydis*; zinc finger transcription factor, cell cycle; appressorium; plant pathogen

**Running title:** Biz1 controls virulence in smut fungus

## **ABSTRACT**

The process of plant invasion involves regulated growth and highly organized morphological changes in many plant pathogenic fungi. For instance, during the infection of corn by the smut fungus *Ustilago maydis*, the dikaryotic infective filament is cell cycle-arrested, and differentiate appressoria prior to plant penetration. Once the filament enters the plant, the cell cycle block is released and the fungal cells start to proliferate. Therefore, a tight interaction between plant invasion and the cell cycle and morphogenesis control systems is predicted. However, there is little information available regarding the relationship of these processes. In this work we describe a novel factor, Biz1 (*b*-dependent zinc finger protein), which plays a pivotal role during the infection process. Biz1 carries two Cys<sub>2</sub>His<sub>2</sub> zinc finger domains and has a nuclear localization suggesting a function as a transcriptional regulator. The deletion of *biz1* does not lead to any detectable phenotypic alterations during axenic growth. However, mutant cells show a severe reduction in appressoria formation and plant penetration, and those hyphae that invade the plant arrest their pathogenic development directly after plant penetration. *biz1* is induced via the *b*-mating type locus which is the key control instance for pathogenic development, and the gene is expressed at high levels throughout pathogenic development. High levels of *biz1* expression induce a G2 cell cycle arrest that is a direct consequence of the down-regulation of the mitotic cyclin Clb1. Our data support a model in which

**Biz1 is involved in the cell cycle arrest preceding plant penetration as well as in the induction of appressoria.**

## INTRODUCTION

Many phytopathogenic fungi are known to differentiate specific infection structures, called appressoria, that facilitate the penetration of the plant epidermal cell layers (Emmett and Parbery, 1975; Deising et al., 2000). In *Magnaporthe grisea*, *Colletotrichum* species and many other plant pathogens, appressoria are visible as discrete, lobed or dome-shaped cells that are separated from the germ tube by a septum. This dome-shaped cell generates enormous turgor pressure and physical force, allowing the fungus to breach the host cuticle and to invade the plant tissue (Mendgen et al., 1996; Talbot, 2003). In smut and rust fungi, appressoria are inconspicuous swellings of the germ tube; it is generally assumed that in these fungi cell wall degrading enzymes, rather than force, aid the penetration of the invading hypha (Gold and Mendgen, 1991). Appressorial development and the penetration step are still poorly understood processes that require the integration of several environmental signals to produce the appropriate differentiation (Dean, 1997). Like other developmental decisions in fungi, appressorium formation must involve regulated growth, control of the cell cycle progression, and highly organized morphological changes.

One of the model systems to investigate the connections between cell cycle and morphogenesis in fungi during plant penetration is *Ustilago maydis*, a basidiomycete causing smut disease on corn plants (Basse and Steinberg, 2004). Haploid cells (sporidia) of this fungus are unicellular, and grow saprophytically by budding. The pathogenic form, the filamentous dikaryon, is established after fusion of two sporidia that have to harbor different alleles of the *a* and *b* mating type loci of *U. maydis*. The *a* locus controls the cell fusion

via a pheromone-receptor based system. Upon pheromone stimulation cells arrest budding growth and start the formation of conjugation tubes (Spellig et al., 1994). These mating filaments undergo directed tip growth towards the pheromone source (Snetselaar et al., 1996), followed by cell fusion and the formation of dikaryotic hyphae. The subsequent steps in filament formation and pathogenic development are controlled by the multiallelic *b*-locus that encodes two distinct homeodomain transcription factors, bE and bW. A heterodimeric complex of the two proteins is formed when they are derived from different alleles, and the presence of this complex is sufficient to initiate pathogenic development (Kahmann and Kämper, 2004).

The dikaryon formed after the fusion of compatible sporidia is arrested in the G2 phase of the cell cycle; for further propagation, it requires plant signals that have not been identified yet. On the plant surface, the filaments differentiate appressoria and penetrate the cuticle (Snetselaar and Mims, 1992, 1993). In contrast to appressoria from other phytopathogenic fungi such as *Magnaporthe grisea* or *Colletotrichum* species (Bechinger et al., 1999; Talbot, 2003), appressoria of *U. maydis* are unmelanized, rather small swellings of the hyphal tip that form penetration structures that are less constricted (Snetselaar and Mims, 1993; Snetselaar et al., 2001). Since it is unlikely that entry of *U. maydis* occurs by mechanical force, it is believed that appressoria simply mark the point at which the growth direction changes. Once the filament enters the plant, cell cycle is reactivated and the fungal cells proliferate to a network of filaments with septated cell compartments each containing a pair of nuclei (Snetselaar and Mims, 1992; Banuett and Herskowitz, 1996).

The morphological changes of *U. maydis* cells during the pathogenic process advocate for tight control of the cell cycle. Previous research efforts have defined networks of regulatory genes that control cell cycle progression (Garcia-Muse et al., 2004; Castillo-Lluva et al., 2004; Castillo-Lluva and Pérez-Martín, 2005; Sgarlata and Pérez-Martín, 2005a, b). As in other eukaryotic organisms, in *U. maydis* cyclin-dependent protein kinases (Cdks) are key regulators of the cell division cycle. Two distinct Cdk-cyclin complexes are responsible for the different cell cycle transitions in *U. maydis*. While Cdk1-Clb1 is required for the G1/S and the G2/M transitions, the Cdk1-Clb2 complex is specific for the G2/M transition (García-Muse et al., 2004). A third Cdk1-cyclin complex composed of Cdk1 and the G1-like cyclin Cln1 regulates the G1/S transition, and has additional functions at the morphogenetic level (Castillo-Lluva and Pérez-Martín, 2005). Regulation of Cdk-cyclin activity throughout the different cell cycle phases is crucial. Inhibitory phosphorylation and activating dephosphorylation of the Cdk1 catalytic subunit are one of the major controls, and we have recently shown that this kind of regulation is crucial for cell cycle progression in *U. maydis* (Sgarlata and Pérez-Martín, 2005a, b). In addition, proteolysis of cyclins is pivotal for cell cycle control. *U. maydis* mitotic cyclins are targeted by the Anaphase Promoting Complex (APC), in association with different adaptor proteins such as Cru1 (Castillo-Lluva et al., 2004) and Cdc20 (Torreblanca and Pérez-Martín, in preparation).

Recently, the role of cell cycle regulators for pathogenic development of *U. maydis* has been addressed. Manipulation of the levels of mitotic cyclins either by affecting their rate of degradation or by alteration of their transcriptional regulation produce fungal cells that are unable to infect the plant (Garcia-Muse

et al., 2004; Castillo-Lluva et al., 2004; Castillo-Lluva and Pérez-Martín, 2005).

These results stress the importance of a tight regulation of the Cdk-cyclin complexes through the pathogenic development of *U. maydis*.

In this work we describe a novel transcriptional regulator, Biz1 (*b*-dependent zinc finger protein), that functions as a repressor for the mitotic cyclin Clb1. *biz1* is induced after initiation of pathogenic development. The deletion of *biz1* does not lead to any detectable phenotypic alterations during axenic growth. However, strains deleted for *biz1* are completely apathogenic. The mutant cells show a low frequency of appressoria formation, and those that produce appressorium and invade the plant arrest their pathogenic development directly after plant penetration.

## RESULTS

### High levels of *biz1* expression induce a G2 cell cycle arrest

In order to isolate novel regulators for the control of cell cycle and morphogenesis during pathogenic development, we performed a genetic screen devoted to the isolation of mutants affected in cell cycle arrest and/or polarity induction in response to pheromone stimulation (See Supplementary Data for a description of such a genetic screen). Serendipitously, in this screen we found that an open reading frame of 783-amino acids -that corresponds to the predicted hypothetical protein um02549 annotated at the MIPS *Ustilago maydis* data base (MUMDB; <http://mips.gsf.de/genre/proj/ustilago/>)- was able to induce cell cycle arrest and strong polar growth in cells expressing it (see below). We called the gene *biz1* (*b*-induced zinc finger, see below).

To analyze the functions of Biz1, we examined the effects of increased expression of *biz1*. For this, we replaced the endogenous promoter within the *biz1* locus with the carbon-source regulated *crg1* promoter (which is repressed by glucose and induced by arabinose, Bottin et al., 1996). The resulting *biz1<sup>crg1</sup>* allele shows a clear carbon-source dependent pattern of expression (Figure 1A). Under repressing conditions (YPD), cells harboring the *biz1<sup>crg1</sup>* allele were morphologically indistinguishable from wild-type strains. However, after transfer to arabinose-containing medium (YPA), cells expressing high levels of *biz1* started to elongate (Figure 1B). We found that these elongated cells contained a single nucleus and long microtubules that reached to the tip of the growing pole (Figure 1D). This polar growth phenotype has been described for *U. maydis* cells arrested in the G2 phase (Steinberg et al., 2001; Banuett and Herskowitz, 2002). Consistently, FACS analysis revealed that the cells have a 2C DNA content (Figure 1C). We did not observe cell divisions after induction of *biz1<sup>crg1</sup>*. Prolonged incubation (more than 24 hours) under inducing conditions resulted in long filaments in which only the tip cell was filled with cytoplasm, and the remaining part of the hyphae consisting of empty sections separated by septa (Figure 1E). Strikingly, these hyphae are reminiscent of the growth mode of the dikaryotic hyphae produced after mating. Under these conditions, cell division is arrested and cells show permanent polarized growth (Steinberg et al., 1998). We believe that this growth mode of *U. maydis* could be a default response to an arrested cell division. For instance, the conditional removal of *clb1*, encoding a mitotic cyclin, led to the same phenotype (García-Muse et al., 2004).



### **Biz1, a putative zinc-finger transcription factor in *U. maydis*.**

The predicted Biz1 protein contains two putative zinc finger domains of the Cys<sub>2</sub>His<sub>2</sub> class, one of the most common DNA binding motifs found in Eukaryota. The two zinc fingers were designated Zf1 (from residues 159 to 183) and Zf2 (from residues 186 to 211). Both are predicted to be composed of two short beta strands ( $\beta$ 1 and  $\beta$ 2) separated by a cysteine-containing short loop (L1), followed by a second loop (L2) and an alpha helix (H) (Figure 2A). While Zf2 comprises the CysX<sub>2-4</sub>CysX<sub>12</sub>HisX<sub>3-5</sub>His consensus for Cys<sub>2</sub>His<sub>2</sub> zinc fingers (Jacobs, 1992), the two cysteine residues in Zf1 are separated only by a single amino acid (Figure 2A). Both zinc fingers contain a conserved hydrophobic residue, a methionine, at position 4 of the proposed  $\alpha$ -helix. The phenylalanine residue at position 3 in the second beta strand ( $\beta$ 2) is a frequent, but not essential feature of Cys<sub>2</sub>His<sub>2</sub> zinc fingers (Suzuki et al., 1994). We have been unable to find any significant sequence similarity between the Biz1 protein and other entries in the databases outside the zinc finger region. Analysis of the amino acid sequence using PROSITE indicated a glutamine-rich region located between residues 507-526, a serine-rich region located between residues 655-702 and a putative nuclear localization signal located upstream of the first zinc finger (residues 145-150). PSORT (Nakai and Horton, 1999) predicts for Biz1 a high probability for nuclear localization (p=94,1). To verify the sub-cellular location, we expressed a Biz1-GFP fusion protein under the control of the arabinose inducible *crg1* promoter (Bottin et al., 1996) in the *U. maydis* haploid wild type strain FB1 (*a1b1*). Fluorescence microscopy revealed bright signals in the nucleus upon induction of the fusion protein (Figure 2B). Induction resulted

in filament formation comparable to that of the cells expressing wild type Biz1, indicating that the GFP fusion did not render the protein inactive.

The presence of two conserved Cys<sub>2</sub>His<sub>2</sub> class zinc finger domains in the predicted sequence of Biz1 suggest a role as transcriptional factor. However, we cannot rule out other functions, as it has been shown that Zn-centered domains can be involved in protein-protein interaction in other proteins than transcriptional regulators (Matthews and Sunde, 2002). To gain support for a role of Biz1 as a transcription factor, firstly we tried to show that the NLS and Zn fingers are required for the function of Biz1. For this, we expressed a N-terminal truncated protein lacking the NLS and zinc finger-containing region fused to a triple HA tag at the C-terminus (Figure 2C). As control we also expressed a carboxy terminal-tagged full-length protein. Both proteins were detected by Western blot assay using anti-HA antibodies (Figure 2C). The addition of a C-terminal triple HA tag did not affect the activity of Biz1, as high levels of the full-length protein induced the already observed cell cycle arrest and hyperpolarized growth (Figure 2D). Strikingly, the N-terminal deleted mutant produced no effect supporting a role of the N-terminal end carrying the NLS and the zinc fingers in the activity of the Biz1 protein.

Taken together, the presence of two Cys<sub>2</sub>His<sub>2</sub> zinc fingers and a glutamine rich region, two features that frequently associate to transcription factors (Escher et al., 2000), as well as the nuclear localization suggest that Biz1 probably functions as a transcription factor.

### **Biz1 down-regulated the expression of the mitotic cyclin *clb1***

In *U. maydis* cells, entry into mitosis from G2 phase requires the activity of two B-type cyclins, Clb1 and Clb2, that form a complex with the catalytic subunit Cdk1 (García-Muse et al., 2004). Since *biz1* overexpression inhibits the G2/M transition, we wondered whether Biz1 could control the expression of these cell cycle regulators via a function as transcriptional regulator. For this, we analyzed the expression of *cdk1*, *clb1*, and *clb2* in *biz1<sup>crg1</sup>* cells and in wild-type cells after 5 hours growth under non-inducing (YPD) and inducing (YPA) conditions. Remarkably, we observed a clear decrease in *clb1* expression under conditions of *biz1* overexpression (Figure 3A). Furthermore, a time-course analysis of *clb1* expression after *biz1* induction showed a strict inverse correlation between the *biz1* and *clb1* mRNA levels (Figure 3B).

Each zinc finger binds a single zinc ion that is sandwiched between the two-stranded  $\beta$ -sheet and the  $\alpha$ -helix, producing a compact fold. In this fold, the comparison of the known structures between zinc finger and DNA target reveals that the vast majority of the base-specific contacts in the zinc finger-DNA complexes are made from positions -1, 2, 3, and 6 of the  $\alpha$ -helix (presumably because these residues are the most prominently exposed on the surface of the helix). The zinc fingers present in Biz1 have a good level of conservation in these residues with respect to well-known zinc fingers which structure of protein-DNA complexes have been described (Wolfe et al., 1999). In addition, the linker region that connect neighboring zinc fingers, which is an important structural element that control the spacing of the fingers along the DNA site, show the most common arrangement composed of five residues between the final histidine of one finger and the first conserved aromatic of the next finger. These similarities made possible to assign a putative sequence recognized by

the zinc fingers of Biz1 (Figure 3C) in basis of the described docking arrangements of previously known zinc finger-DNA structures (Wolfe et al., 1999; Paillard et al., 2004). Search of putative recognition sites in the regulatory upstream sequence of *clb1* indicated six hits with a single mismatch (Figure 3D). We sought to analyze whether Biz1 is associated to the *clb1* regulatory region. For this, we made use of chromatin immunoprecipitation, a method that measures the extent to which certain genomic DNA regions can be cross-linked to a specific protein under in vivo conditions (Hecht et al., 1999). Biz1 was provided as a carboxy-terminal HA epitope-tagged protein or untagged protein as control. Cross-linked protein-DNA complexes were immunoabsorbed and selected stretches of coprecipitated DNA were amplified by PCR and analyzed by gel electrophoresis. We used primers that amplified promoter regions of *cdk1* and *clb2* as negative controls (since their mRNA levels were unaffected by high dose of Biz1), and three different primer pairs to amplify the *clb1* upstream region. We observed that amplification of the upstream *clb1* region can be obtained, while a weakly or not at all amplification was obtained from control promoters (Figure 3E). Strikingly the amplification signal of *clb1* promoter was obtained only with the distal regions, where the putative Biz1-recognition sites were located.

### **Down-regulation of *clb1* expression accounts for the cell cycle arrest induced by *biz1* overexpression**

Clb1 forms a complex with Cdk1 and, together with the Clb2-Cdk1 complex, is required for the G2/M transition in *U. maydis* (Garcia-Muse et al., 2004). Therefore, the observed G2 arrest after *biz1* expression could be well explained

by the decrease in *clb1* mRNA levels. Alternatively, the decrease of *clb1* mRNA level could be a consequence and not the cause of the G2 cell cycle arrest. We reasoned that if ectopic *clb1* expression circumvents the Biz1-induced cell cycle arrest, it would imply that transcriptional down-regulation of *clb1* is the cause of the cell cycle arrest. Alternatively, a cell cycle arrest regardless of the promoter driving *clb1* expression would suggest that the observed down-regulation of *clb1* is simply a consequence of the Biz1-induced cell cycle arrest. To address this question, we took advantage of a *U. maydis clb1<sup>nar1</sup>* strain, in which the native *clb1* promoter was replaced with the *nar1* promoter (García-Muse et al., 2004). The cells of this strain show a wild-type phenotype when grown under conditions where the *clb1<sup>nar1</sup>* gene is expressed (minimal medium amended with nitrate as nitrogen source, García-Muse et al., 2004). We introduced the *biz1<sup>crg1</sup>* allele into the *clb1<sup>nar1</sup>* strain and grew these cells under conditions where *clb1<sup>nar1</sup>* is expressed (nitrate) and either non-induced (glucose) or induced (arabinose) conditions for *biz1<sup>crg1</sup>* expression. As expected, *biz1* induction led to the repression of the native *clb1* gene, while the expression of the *clb1<sup>nar1</sup>* gene was not altered (Figure 4A). In the latter case, no cell cycle arrested cells were observed, even after prolonged incubation (Figures 4B and 4C). These data indicate that down-regulation of *clb1* expression by Biz1 is the cause of the observed cell cycle arrest.

### **Biz1 is required for virulence**

To investigate the physiological role of *biz1*, null mutants were constructed by one-step replacement in the haploid wild-type strains FB1 (*a1b1*) and FB2 (*a2b2*). When grown in liquid culture, the deletion strains showed no obvious

phenotypic alterations to wild type cells with respect to morphology (Figure 5A) and cell cycle profile (Figure 5B) or growth properties in various media (not shown). To assay mating competence, FB1 $\Delta$ *biz1* and FB2 $\Delta$ *biz1* were co-cultivated on charcoal-containing agar plates. Under these conditions, compatible wild-type strains fuse and develop filamentous dikaryotic hyphae that can be recognized as white fuzzy mycelium (Day and Anagnostakis, 1971). In wild-type strains, these filaments are cell cycle arrested and consist of a single binucleated tip cell that leave empty, septated cell compartments behind (Steinberg et al., 1998). *biz1*-mutant crosses formed filaments similar to those observed in wild-type crosses (Figure 5C), and microscopic observation showed no difference in the morphology of the filaments. However, nuclear staining with 4',6-diamidino-2-phenylindole (DAPI) revealed a higher frequency of filaments carrying more than two nuclei in the mutant crosses, suggesting a defect in the ability to arrest mitosis during the formation of the infective hyphae (Figures 5D and 5E).

To assess the role of *biz1* in pathogenesis, plants were inoculated with a mixture of the compatible FB1 $\Delta$ *biz1* and FB2 $\Delta$ *biz1* strains. Infection with the respective wild-type strains led to tumor production in 89% of the inoculated plants. In contrast, in infections with the mutant strains no plant tumors were obtained (Table 1). Only in a few occasions, chlorosis around the inoculation point was observed.

Taken together these results illustrate that Biz1 is a factor specifically required for pathogenic development of *U. maydis*.

**The absence of *biz1* impairs appressorium formation and proliferation of the fungus in the plant tissue.**

To elucidate at which stage pathogenic development of the mutant strain is blocked, the early infection process was followed using a  $\Delta biz1$  derivative of strain SG200. SG200 harbors a compatible combination of the *bE1* and *bW2* genes and the *mfa2* gene inserted in the *a1* locus and is thus able to infect plants without the need for a mating partner (Bölker et al., 1995). Similar to the cross of  $FB1\Delta biz1$  and  $FB2\Delta biz1$ ,  $SG200\Delta biz1$  forms filaments on charcoal plates (Figure 6A) and is a pathogenic (Figure 6B, Table 1). After plant inoculation, fungal cells on the plant surface were stained with Calcofluor. We observed vigorous filament formation on the plant surface both in SG200 and  $SG200\Delta biz1$  infections (Figure 6C, upper row).  $SG200\Delta biz1$  was able to form appressoria with morphology comparable to that of the wild type SG200 filaments (Figure 6C, bottom row). However, we noticed a decrease in the number of appressoria produced by the mutant strain. A decrease in the ability to form appressoria has also been noted in infections with mixtures of compatible haploid *biz1* mutants versus wild-type strains (not shown).

To allow the quantitative comparison of appressoria formation, we co-infected plants with equal numbers of SG200 and  $SG200\Delta biz1$  cells that were tagged with constitutively expressed genes for the Cyan Fluorescent Protein (CFP) or Yellow Fluorescent Protein (YFP), respectively (Figure 6D). We found that irrespective of the combination used (i.e.  $SG200::CFP$  and  $SG200\Delta biz1::YFP$  or  $SG200::YFP$  and  $SG200\Delta biz1::CFP$ ), appressoria formation was reduced at least 10 fold in  $\Delta biz1$  cells when compared to wild-type cells (Figure 6E). These

results indicate a role of Biz1 in appressorial structures formation on the plant surface.

In the few cases where appressoria were produced in SG200 $\Delta$ *biz1* cells, Chlorazole Black E staining was used to visualize invading hyphae (Brachmann et al., 2003). Strikingly, mutant hyphae arrested growth after penetration of the plant surface and did not extend growth beyond the epidermal cell layer (Figure 7A). Supporting the defect in the progression through plant tissue, we found that hyphae entering via the natural opening provided by stomata were unable to progress through the plant tissue either (Figure 7B).

### ***biz1* is a *b*-regulated gene that is highly expressed during the infection process**

In agreement with the absence of phenotypic alterations in  $\Delta$ *biz1* cells under axenic conditions, *biz1* expression was barely detectable in haploid strains growing in liquid culture (for instance, see Figure 1A). Since *biz1* is required for virulence, it was likely that its expression would be activated under conditions that induce the pathogenicity program. Thus, we analyzed the *biz1* expression in strains with activated *a*- and *b*-pathways that were grown on charcoal-containing agar plates, a condition that mimics the plant surface with respect to the ability to induce the mating determinants (Holliday, 1974). We used the wild-type haploid strain FB1 (*a1b1*), mixtures of FB1 (*a1b1*) and FB2 (*a2b2*), the solopathogenic haploid strain SG200 (*a1mfa2bW2bE1*), and the solopathogenic diploid strain FBD11 (*a1ab1b2*). Northern analysis confirmed a low level of *biz1* expression in the wild-type haploid strain. However, all strains with compatible *a*- and *b*-mating type combinations and a thus activated pathogenic program



(mixture of FB1 and FB2, FBD11, SG200), displayed a clearly induced *biz1* expression (Figure 8A). In the diploid strain FBD12-3 (*a1a2b1b1*), where pheromone signaling is constitutive and an active *b* complex is missing, no *biz1* expression was present. Furthermore, haploid cells expressing an activated form of the MAPK kinase Fuz7 (Fuz7DD, Müller et al., 2003) and therefore mimicking an active pheromone signaling, do not express *biz1* either (Figure 8B). On the contrary, in the haploid strain AB33 (Brachmann et al., 2001), harboring the compatible *bW1/bE2* genes under the control of the nitrate inducible *nar1* promoter (Brachmann et al., 2001), a strong *biz1* induction is observed in nitrate containing medium, whereas in the control strain AB34, harboring the non-compatible *bE2/bW2* combination, only a faint signal is detectable under the same conditions (Figure 8B). Thus, we conclude that *biz1* expression is independent from the *a*-locus mediated pathway and strictly dependent on the presence of an active *bE/bW* heterodimer.

To analyze *biz1* expression during pathogenic development, corn plants were inoculated with a mixture of FB1 and FB2 cells, infected leaf areas were collected at different time points, and RNA was extracted and submitted to RT-PCR analysis (Figure 8C). We found that *biz1* is expressed at all stage during pathogenic development. Although  $\Delta$ *biz1* mutants arrest early during infection, the observed expression at later stages suggests additional roles for the Biz1 beyond the penetration step.

### **High level of Clb1 interferes with infective filament formation**

We wondered whether the *biz1*-dependent regulation of *clb1* could account for the penetration defect observed in  $\Delta$ *biz1* strains. Constitutive high levels of

mitotic cyclins interfere with pheromone signaling and, as a consequence, hinder the induction of the *bE* and *bW* genes, resulting in decreased virulence (Castillo-Lluva et al., 2004; Castillo-Lluva and Pérez-Martín, 2005). In addition, the inability to control cyclin levels inside the plant affects the infection process (Castillo-Lluva et al., 2004). To circumvent these interferences, we took advantage of the *dik6* promoter. *dik6* expression is dependent on the bE/bW heterodimer (Brachmann et al., 2001); the gene is strongly expressed in hyphae growing on the plant surface but it is down-regulated once the hyphae have penetrated the plant (G. Weinzierl and J. Kämper, unpublished). Therefore, to achieve high *clb1* mRNA levels specifically during the stage of infection where the appressoria are formed, we introduced *clb1* under the control of the *dik6* promoter ( $P_{dik6}:clb1$ ) into SG200. In this strain, the  $P_{dik6}:clb1$  fusion should lead to the reversion of the negative regulation of *clb1* by *biz1* once the *b*-dependent program is activated. In SG200  $P_{dik6}:clb1$  cells grown on charcoal-containing agar plates (conditions in which the *bE* and *bW* genes are highly expressed), a strong induction of *clb1* was observed. SG200 cells grown under the same conditions show only a weak *clb1* expression (Figure 9A). This decrease is not totally dependent on *biz1*, since in SG200 $\Delta$ *biz1* cells there is still some level of *clb1* down-regulation in charcoal-containing plates with respect to CMD plates, indicating that additional factors are involved in the regulation of *clb1* during the initial steps of pathogenic development. Since *clb2* expression seems not to be affected by *biz1* expression, we also checked the level of *clb2* mRNA as a control (Figure 9A).

Strikingly, cells carrying the ectopic  $P_{dik6}:clb1$  transgene showed a clear decrease in the ability to form filaments on charcoal plates: aerial hyphae were

observed as a much thinner layer of filaments in the colony (Fig 9B). Microscopic analysis of the cells within the colony revealed that about 80% of these cells displayed an aberrant morphology and were carrying several nuclei (Figure 9C), suggesting a defect in the cell cycle arrest associated with the formation of infective filaments. However, it was also possible to detect filaments with wild-type morphology and single nuclei. Despite of the clear impairment in filament formation, SG200 *P<sub>dik6</sub>:clb1* cells were able to infect corn plants, although with lower efficiency (Table 1). Therefore, we analyzed the ability of SG200 *P<sub>dik6</sub>:clb1* cells to form appressoria on corn leaves. Similar to the situation on CM-charcoal plates, the majority of the cells *on planta* displayed an aberrant morphology, and a minority of filaments exhibited wild-type morphology (not shown). Remarkably, appressorium formation on plant surface was only observed for the filaments with wild type-like appearance and a single nucleus (Figures 9D and 9E), suggesting that only cells able to arrest the cell cycle are competent to produce appressoria.

## DISCUSSION

In this study, we have identified a new factor, Biz1, which is required for pathogenic development of *U. maydis*. Biz1 also has impacts on cell cycle control via the down-regulation of the gene for the mitotic cyclin Clb1.

The predicted Biz1 protein contains two conserved nucleic acid-binding Cys<sub>2</sub>His<sub>2</sub> zinc finger domains and a glutamine rich region that is known from several eukaryotic transcription factors such as Sp1 or Oct1 to mediate transcriptional activation (Escher et al. 2000). Consistent with the prediction from PSORT, Biz1 shows a nuclear localization. We found that the N-terminal

half of Biz1, carrying the zinc fingers as well as the nuclear localization signal, is required for its activity. In addition, using chromatin immunoprecipitation assays we have been able to show a physical interaction between Biz1 and the upstream regulatory region of *clb1*. Thus, we favor that Biz1 is a transcription factor. A limited number of transcriptional regulators have been described associated with virulence in phytopathogenic fungi. In *Fusarium oxysporum*, the Cys<sub>2</sub>His<sub>2</sub> zinc finger transcription factor PacC, a conserved regulator involved in pH sensing, is required for virulence (Caracuel et al., 2003). In *Claviceps purpurea*, the CREB-like transcription factor CPTF1 is involved in oxidative stress response, and deletion of CPTF1 leads to reduced virulence (Nathues et al., 2004). ToxE is a pathway specific transcription factor essential for the expression of HC-toxin required for pathogenicity of *Cochliobolus carbonum* (Pedley and Walton, 2001). Finally, in *Magnaporthe grisea*, Mst12, a Ste12 homologue, was found to be essential for penetration and invasive growth (Park et al., 2002). However, Biz1 function cannot be related to that of any of these known transcription factors, although the *biz1* deletion, similar to the phenotype observed for the *MST12* deletion in *M. grisea*, leads to a penetration defect. However, while a *MST12*Δ strain in *M. grisea* is not impaired in appressoria formation, in *U. maydis* Δ*biz1* strains the frequency of appressoria formation is dramatically reduced.

The *biz1* gene is not expressed in haploid wild-type cells, and deletion analysis revealed no function for *biz1* during saprophytic growth. *biz1* expression is strictly dependent on the presence of a bE/bW heterodimer; induction of the a-pathway either by pheromone or by a constitutive active MAPK-cascade (Fuz7DD) does not show any effects. It has been proposed that the bE/bW

heterodimer triggers a regulatory cascade in which class 1 genes are directly regulated by the binding of the bE/bW heterodimer to a conserved DNA motif termed *bbs* (*b* binding sequence) in the upstream region of *b* responsive genes, and class 2 genes are indirectly regulated by *b* via yet unidentified regulatory proteins that are encoded by class 1 genes (Romeis et al, 2000; Brachmann et al., 2001). In the promoter region of *biz1*, we could not detect any *bbs* motif, and we observed a delayed expression of *biz1* after bE/bW induction during time-course experiments (not shown). Furthermore, compared to the expression observed after *b*-induction in charcoal-containing plates, *biz1* expression increased at least 4-fold after the fungus has penetrated the plant, suggesting additional factors favoring *biz1* expression specific for *in planta* conditions. Thereby, we favor the idea that *biz1* is regulated indirectly via a *b*-dependent signaling cascade that allows the input of additional environmental cues for its regulation. It is conceivable that such cues must be perceived already on the plant surface.

In wild-type cells, after cell fusion, the assembly of a compatible bE/bW heterodimer induces the formation of a cell cycle-arrested dikaryotic filament that is characterized by tip growth and the generation of empty sections in the distal parts of the filament (Steinberg et al., 1998). Mutants lacking Biz1 were able to form this infectious filament, although an increase in filaments carrying more than two nuclei (i. e. not cell cycle arrested) was observed. Strikingly, ectopic expression of *biz1* in axenic conditions resulted in a G2 cell cycle arrest. We were able to show that *clb1*, encoding a mitotic cyclin essential for G2/M transition, was down-regulated by Biz1. We also demonstrated that the cell cycle arrest is a direct consequence of the down-regulation of *clb1* expression.

Since Biz1 seems to be positively regulated by the *b* locus and since high levels of Biz1 protein arrest the cell cycle, it is tempting to speculate that Biz1-mediated down-regulation of *clb1* expression is responsible for the *b*-dependent cell cycle arrest. Moreover, the results obtained after reprogramming *clb1* expression during the induction of the infective filament using the *dik6* promoter supports the importance of *clb1* down-regulation for a correct formation such a structure. However, additional control systems ensuring a cell cycle arrest must exist, since deletion of *biz1* or over-expression of *clb1* do not completely abolish the formation of the typical cell cycle-arrested hyphae. Such additional controls may well involve inhibitory phosphorylation of the Cdk1 kinase by the Wee1 kinase. We recently reported that over-expression of Cdc25, a phosphatase that counteracts the Wee1-mediated inhibition of Cdk1, impairs the formation of *b*-dependent filaments (Sgarlata and Pérez-Martín, 2005b). We believe that complementary and somehow redundant mechanisms, such as down-regulation of cyclin expression and direct inhibition of kinase activity (i. e. by inhibitory phosphorylation), could be responsible of the *b*-induced cell cycle arrest. Biz1 is one of the factors responsible for the cyclin down-regulation, although not the only one. We based this conclusion in two results: firstly, the dramatic difference between SG200 $\Delta$ *biz1* and SG200  $P_{dik6}::clb1$  cells to form cell cycle-arrested filaments advocates for additional factors that could down-regulate *clb1* expression during pathogenic development; secondly in SG200 $\Delta$ *biz1* cells growing on charcoal medium (and thus having an elevated level of *b*-expression), *clb1* is down-regulated (although to a lesser extend than in the wild-type situation). Further research efforts will be needed to define the

nature of these putative additional mechanisms of *b*-dependent cell cycle control.

Is cell cycle arrest connected to appressorium formation? We observed that in the reprogrammed SG200  $P_{dik6}:clb1$  strain appressorium formation is always associated cell cycle-arrested filaments, but never to aberrant non-arrested cells. On the other hand, SG200 $\Delta biz1$  was able to produce cell cycle-arrested filaments, but only low numbers of appressoria were detected. Taken together, these two observations suggest that cell cycle arrest is necessary, but not sufficient for appressorium formation. It is conceivable that during appressorium development the response to external cues (i. e. signals from plant surface) as well as internal cues (i. e. cell cycle arrest) must be timely coordinated. A delay in the sensing of either external or internal cues (for instance a delay in cell cycle arrest) could therefore lead to an inefficient response and thus result in impaired appressorium formation. The importance of precise connections between cell cycle regulation and appressorium formation has been recently highlighted in the rice blast fungus, *Magnaporthe grisea*, where it has been proposed that either a G2/M or a postmitotic checkpoint may regulate appressorium formation (Veneault-Fourrey et al., 2006).

The arrested cell cycle of the infective hyphae is released once the fungus enters the plant. Consistently, we found that *clb1* is expressed inside the plant (unpublished observations). As *biz1* is expressed during the biotrophic phase, there must be additional factors that uncouple the *clb1* down-regulation from Biz1, once the fungus penetrates the plant. These still uncharacterized factors are expected to have an essential role during the infection process.

Finally, we believe that cell cycle arrest and appressorium formation are not the only processes controlled by Biz1 during the infection process. Since *biz1* is expressed during the entire biotrophic phase, it is conceivable that the protein fulfils additional roles at this stage. We found that in the rare occasions that *biz1*-defective cells penetrate the plant surface either by producing appressoria or by using the natural opening provided by stomata, the fungus was unable to proliferate inside the plant, corroborating the importance of Biz1 for fungal development after penetration. In the future, the characterization of genes regulated by Biz1 will provide insights to understand these proposed downstream roles.

## **METHODS**

### **Strains and growth conditions**

*Ustilago maydis* strains are derived from FB1 (*a1b1*) (Banuett and Herskowitz, 1989) and are listed in Table 2. Cells were grown at 28°C in YPD (Sherman et al., 1986), complete medium (CM) or minimal medium (MM) (Holliday, 1974). Controlled expression of genes under the *crg1* and *nar1* promoters were performed as described previously (García-Muse et al., 2004; Brachmann et al., 2001). FACS analysis was described previously (García-Muse et al., 2003). Mating assays and plant infections were carried out as described (Gillissen et al., 1992).

### **DNA and RNA analysis**

*U. maydis* DNA isolation was performed as previously described (Tsukuda et al., 1988). RNA isolation from axenic cultures, charcoal plates and plant tissues



were performed as described (Basse et al., 2002). Northern analysis was performed as described previously (Garrido and Pérez-Martín, 2003). A 579 bp DNA fragment spanning the sequence coding the first 193 amino acids of Biz1 was used as probe. The *cdk1*, *clb1* and *clb2* probes were already described (García-Muse et al., 2004). A 5'-end labeled oligonucleotide complementary to the *U. maydis* 18S rRNA (Bottin et al., 1996) was used as loading control in Northern analyses. A phosphorimager (Molecular Imager FX, Bio-Rad) and the suitable program (Quantity One, Bio-Rad) were used for visualization and quantification of radioactive signals.

First-strand cDNA synthesis was performed using the SuperScript III First strand synthesis SuperMix assay (Invitrogen) according to the manufacturer's protocol. 1µg of total RNA was used as a template for the reaction. Samples were incubated at 50°C for 50 min. Real-time PCR was performed on a Bio-Rad iCycler system using the Platinum SYBR Green qPCR SuperMix-UDG (Invitrogen) according to the manufacturer's protocol. Cycling conditions were as follows: 95°C for 2 min, 45 cycles of 30 s at 95°C, 30 s at 62°C and 30 s at 72°C. After each PCR, the specificity of the amplifications was verified and the threshold cycle above background was calculated using the Bio-Rad iCycler software. The gene encoding peptidylprolyl isomerase (*ppi*) was used as a constitutive control for normalization. Relative expression values were calculated using the Bio-Rad Gene Expression Macro. Forward (F) and reverse (R) primers used were as follows: *biz1*: Rt-biz1-F3: 5'GGATCAGCCAAATGATGGACAG3' and Rt-biz1-R3: 5'TACTCTCGCATCTCTTCCACTC3'; *ppi*: 5'Rt-ppi-F2: ACATCGTCAAGGCTATCG3' and Rt-ppi-R2: 5'AAAGAACACCGGACTTGG3'.

### **Plasmid and strain constructions**

Plasmid pGEM-T easy (Promega) was used for cloning, subcloning and sequencing of genomic fragments and fragments generated by PCR. Plasmid pRU11 (Brachmann *et al.*, 2001) was used to express genes under the control of the *Pcrg1* promoter. Sequence analysis of fragments generated by PCR was performed with an automated sequencer (ABI 373A) and standard bioinformatic tools. To construct the different strains, transformation of *U. maydis* protoplasts with the indicated plasmids was performed as described previously (Tsukuda *et al.*, 1988). Homologous recombination of gene replacement into the corresponding loci was verified by diagnostic PCR and subsequent Southern blot analysis.

Deletion of *biz1* in FB1 and FB2 was done by homologous replacement following the protocols of Kämper, 2004 and Brachmann *et al.*, 2004. Briefly, a pair of DNA fragments flanking the *biz1* ORF were amplified and ligated to a hygromycin resistance cassette via *SfiI* sites. The 5' fragment spans from nucleotide -1000 to nucleotide -1 (considering the adenine in the ATG as nucleotide +1) and it was produced by PCR amplification using the primers UST12-2 (5'CTGCATGTTTCGGACGCCAACAATGGGC3') and UST12-3 (5'ATGGCCATCTAGGCCGCTGTTTCAAGCACACTGGCCCTC3'). The 3' fragment spans from nucleotide +2352 to nucleotide +3357, and it was produced by PCR amplification using the primers UST12-6 (5'TAGGCCTGAGTGGCCAGCATGGGCGAAAGCTGACTCGAC3') and UST12-7 (5'CAGCTAGCGATCCTTGACGCCGTTCC3'). To delete *biz1* in SG200 we followed the same strategy; the 5' fragment spans the region from -7

to – 981 (with respect to the ATG), and the 3' fragment spans 1057 bp 3' of the stop codon. Primers used were Biz1-lbn (5'CAATGGGCATGTGCTCTTG3'), Biz1-lb2 (5'GTTGGCCTGAGTGGCCCAAGCACACTGGCCCTCG3'), Biz1-rbn (5'GAAGGGCGTTGAAGGATG3') and Biz1-rb2 (5'GTTGGCCATCTAGGCCGCTGACTCGACTGCCTGC3').

To produce a conditional *biz1<sup>crg1</sup>* allele, we constructed a plasmid by ligation of two fragments into pRU11 digested with *NdeI* and *EcoRI*. The 5' fragment (flanked by *EcoRI* and *BamHI*) was produced by PCR using the primers USTA (5'CGGGATCCTCTTGCGCATCAAAGCTGCGCTG3') and USTB (5'CGGAATTCATGCCAGGTAGTCGAGAGCCATC3'). This fragment spans from nucleotide -967 to nucleotide -256 (considering the adenine in the ATG as nucleotide +1). The 3' fragment (flanked by *NdeI* and *BamHI*) was obtained by PCR amplification with primers UST12-4 (5'CATATGTCGATGCTTAGCACACGGGCA3') and UST12-5 (5'CCGGAATTCCCAACGACGGCTGTGGTGACC3') and spans from nucleotide +1 to nucleotide +2360. The resulting plasmid pBIZ1crg was integrated, after digestion with *BamHI*, by homologous recombination into the *biz1* locus.

To construct the *P<sub>dik6</sub>:clb1* allele, a 2,1 Kb *NdeI-NotI* fragment from pRU11-CLB1 (García-Muse et al., 2004) carrying the *P<sub>crg1</sub>* promoter was exchanged with a PCR amplified 1,1 Kb *NdeI-NotI* fragment carrying the *P<sub>dik6</sub>* promoter (Sgarlata and Perez-Martin, unpublished). The resulting plasmid pCLB1dik6 was integrated, after digestion with *SspI*, by homologous recombination into the *cbx* locus as described previously (Brachmann et al., 2001).

To produce a *biz1-gfp* fusion, a PCR-generated 2,3 kb *NdeI* fragment carrying the *biz1* ORF without the stop codon was inserted at the single *NdeI* site of pRU11 (Brachmann et al., 2001), allowing the fusion at the C-terminal end of Biz1 with GFP and an expression under control of *crg1* promoter. This construction was integrated, after digestion with *XcmI*, by homologous recombination into the *cbx* locus as described previously (Brachmann et al., 2001).

To produce the *biz1-HA* and *biz1 $\Delta$ 218-HA* alleles under the control of the *crg1* promoter, the *biz1* ORF was amplified using UST12-4 (that amplifies from the first ATG; 5'CATATGTCGATGCTTAGCACACGGGCA3') or Biz1 $\Delta$ ZF (that amplifies from nucleotide +652; 5'CATATGCGAACCACGGCTTCCATGTC3') and UST12-5 (that amplifies until the end of the ORF without the stop codon; 5'GAATTCCCAACGACGCCTGGTGTGACC3'). The corresponding fragments were cloned as *NdeI-EcoRI* into pGNB-HA (a pGEX-2T derivate that carries three copies of the *ha* epitope; Perez-Martin, unpublished), and the resulting tagged alleles were cloned as *NdeI-AflIII* into pRU11 (Brachmann et al., 2001). The pRU11-Biz1HA and pRU11-Biz $\Delta$ 218HA plasmids were integrated, after digestion with *SspI*, by homologous recombination into the *cbx* as described previously (Brachmann et al., 2001).

Plasmids allowing the constitutive expression of *cfp* and *yfp* genes (pOMA-CFP and pOMA-YFP) are based on plasmid pCU4 (Loubradou et al., 2001). In pCU4, the *o2tef* promoter was replaced with a 1.3 kb *SpeI/XmaI* from plasmid pSL1180-OMA with the OMA promoter (C. Aichinger, O. Ladendorf, unpublished) to yield pOMA-GFP. The OMA promoter consists of the *U. maydis mfa1* minimal promoter fused to 8 enhancer elements from the *U. maydis prf1*

gene promoter and leads to strong constitutive expression (C. Aichinger, unpublished). The *NotI* site in the vector backbone in pOMA-GFP was deleted by use of Klenow-polymerase and religation, and subsequently, the *gfp* gene was replaced with *XmaI/NotI* fragments harbouring the *yfp* and *cfp* genes from plasmids pOY and pOC (Weber et al., 2003), respectively. The resulting plasmids pOMA-CFP and pOMA-YFP were integrated into the *cbx*-locus after linearization with *SspI* as described previously (Brachmann et al., 2001).

### **Chromatin Immunoprecipitation Assays**

Chromatin immunoprecipitation PCR assays were performed as described (Hecht et al., 1999). For cross-linking, *U. maydis* cells producing non-tagged or tagged Biz1 protein were treated with 1% formaldehyde for 15 min at room temperature. Chromatin was sheared by sonication to an average size of 1000 bp. Primer sequences utilized are described in Supplementary Table 1.

### **Microscopic observations**

Microscopy was carried out either using a Leica DMLB microscope or a Zeiss Axioplan 2. Phase contrast or standard FITC and DAPI filter sets were used for epifluorescence analysis of nuclear staining with DAPI (García-Muse *et al.*, 2003), WGA and calcofluor staining, performed as described (Castillo-Lluva and Pérez-Martín, 2005). Photomicrographs were obtained with a Leica 100 or AxioCam HrM camera and the images were processed with Axiovision (Zeiss) and Photoshop (Adobe).

## Sequence analyses

Predicted amino acid sequences were analyzed using the programs BLAST (Altschul et al., 1997) and PSORT (Nakai and Horton, 1999).

## ACKNOWLEDGEMENTS

We wish to thank Prof. Holloman (Cornell University, New York) for the gift of the pCM54-based *U. maydis* gene library; Jan Schirawski (MPI, Marburg) is acknowledged by his generous gift of wild-type fungus infecting the plant through stomata. This work was supported by a Grant from the MCyT (BIO2005-02998) and a EU contract (MRTN-CT-2005-019277) to J. P.-M., and by a grant of the German BMBF to J.K.; I. F.-P. was a recipient of a FPI fellowship from the MCyT. M. V. was supported by a grant from the International Graduate School GRK767 funded by the German Research Foundation (DFG).

## LEGENDS TO FIGURES

**Figure 1.** Expression of *biz1* arrests the cell cycle in G2 phase

**(A)** Arabinose-induced expression of *biz1*. The wild type FB1 and conditional UMN53 (FB1*biz1*<sup>crg1</sup>) strain were grown for 6 hours in non-inducing conditions (YPD, glucose) or inducing conditions (YPA, arabinose). The RNA was extracted and analyzed by Northern blotting, loading 10 µg total RNA per lane. A probe specific for 18s rRNA was used to control for loading.

**(B)** Micrographs showing the cell morphology of UMN53 cells after 12 hours of growth in YPD (non-inducing conditions) or YPA (inducing conditions) liquid

cultures. Note the elongated shape, and the presence of a single nucleus (DAPI staining). Bar 20  $\mu\text{m}$ .

**(C)** FACS analysis of FB1 and UMN53 (FB1*biz1*<sup>crg1</sup>) to assess DNA content in non-inducing (YPD) and inducing conditions (YPA). Samples were taken at 0,3, 6 and 9 hours after transfer to inducing conditions. Cells expressing *biz1* arrest their growth at G2 and thereby accumulate with a 2C DNA content. The shift to DNA content higher than 2C observed in UMN53 cells incubated in YPA for 9 hours was due to mitochondrial DNA staining.

**(D)** Microtubule network in UMN68 cells, carrying a  $\alpha$ -tubulin-GFP fusion and expressing high levels of *biz1* after 8 h in YPA (Tub1-GFP: epifluorescence). Bar 20  $\mu\text{m}$ .

**(E)** UMN53 cells incubated for 24 hours in inducing conditions display a distinct phenotype characterized by a extensive polarized growth (upper horizontal panel, DIC), single nuclei content (DAPI, arrow point to the nucleus) and empty sections behind that are separated by septa (stained with wheat germ agglutinating, WGA, arrows) generated by formation of basal vacuoles, as result of a permanent G2 cell cycle arrest. Vertical panel shows a detailed view of the basal area of the hypha, where the septa-separated empty sections can be observed. Bars in horizontal panels, 50  $\mu\text{m}$ ; bar in vertical panel 15  $\mu\text{m}$ .

**Figure 2.** *biz1* encodes a zinc finger-containing protein.

**(A)** Domain structure of Biz1. Domains indicated were identified using PROSITE. Biz1 contains a nuclear localization signal (NLS), a glutamine-rich region, a serine-rich region and two zinc fingers. The lower part shows the sequence of the two putative Cys<sub>2</sub>His<sub>2</sub> zinc finger domains; amino acids

predicted to be involved in the formation of the  $\beta$  strands ( $\beta 1$  and  $\beta 2$ ), the loops (L1 and L2) and the  $\alpha$  helix (H) are indicated. Residues corresponding to the Cys<sub>2</sub>His<sub>2</sub> zinc finger consensus sequence are in gray tone.

**(B)** The Biz1-GFP fusion protein localizes to the nucleus. Cells harboring an ectopic copy of a *biz1-gfp* fusion under the control of the arabinose inducible *crg1* promoter (UMN68 strain), were grown for 4 hours under inducing conditions (Complete Medium supplemented with 1% arabinose as carbon source). Bar 15  $\mu\text{m}$ .

**(C)** In the upper part, a scheme of the C-terminal tagged Biz1 protein as well as its derivative lacking the NLS and Zinc fingers, Biz1 $\Delta$ 218-HA is showed. In the lower part a Western blot assay to detect Biz1 proteins is showed. Extracts were prepared from FB1 P<sub>crg</sub>:Biz1HA and FB1P<sub>crg</sub>:Biz1 $\Delta$ 218HA grown in inducing conditions (YPA) or repressive conditions (YPD) at OD<sub>600</sub> of 0,5. Equal amount of total protein (50  $\mu\text{g}$ ) were loaded into the gel. Anti-HA-peroxidase (Roche) antibodies were used to detect the fusion proteins. Right bars indicated the molecular masses of the protein marker ladder. Biz1-HA and Biz1 $\Delta$ 218HA have an estimated molecular mass of 88kDa and 64kDa, respectively.

**(D)** Morphology of cells producing the Biz1-HA or the Biz1 $\Delta$ 218HA protein, growing in inducing conditions (YPA). Bar 20  $\mu\text{m}$ .

### **Figure 3.** Biz1 down-regulates *clb1* mRNA levels

**(A)** Expression level of the genes encoding the components of the mitotic cyclin-dependent kinase in *U. maydis*: *cdk1*, *clb1*, and *clb2*. FB1 and UMN53 (FB1*biz1*<sup>*crg1*</sup>) cells were grown in non-inducing (YPD) and inducing (YPA) conditions for *biz1* overexpression in liquid cultures for 8 hours, and the RNA



was extracted and analyzed by Northern blotting, using specific probes for each gene, as indicated on left. 10  $\mu$ g of total RNA was loaded per lane. A probe specific for 18s rRNA was used to control for loading.

**(B)** Induction of *biz1* and its effect on *clb1* expression. UMN53 (FB1*biz1*<sup>crg1</sup>) cells growing in glucose-containing YPD were washed three times and transferred to arabinose-containing YPA, and samples were taken at the indicated times (in hours). RNA was isolated and submitted to RNA gel blot analysis as above.

**(C)** The sequence of the two zinc fingers of Biz1 is shown in the upper part. The secondary structure prediction is also schematized (arrows indicate  $\beta$ -sheet while the box indicates  $\alpha$ -helix). The numbers indicate the position with respect to the putative recognition  $\alpha$ -helix. At the bottom, scheme showing the proposed key amino acid-base contacts from positions -1, 2, 3, and 6 of each  $\alpha$ -helix.

**(D)** Scheme of the promoter region of *clb1* depicting the location of the primers utilized in chromatin immunoprecipitation as well as the location of the different hits of the theoretical recognition sequence for Biz1. The different hits are showed in the lower part of the figure.

**(E)** Association of Biz1-HA with the *clb1* promoter as measured by ChIP. Strains producing non-tagged Biz1 and Biz1-HA tagged proteins were submitted to Immunoprecipitation. Control lanes show DNA amplified from extracts without tagged protein (Biz1) or prior to immunoprecipitation (whole-cell extract, WCE). The following primer pairs were used: *cdk1*: CDK1-5/CDK1-7; *clb2*: CYC2-1/CYC2-3; *clb1A*: ChIP1/ChIP2; *clb1B*: ChIP3/ChIP4; *clb1C*: ChIP5/ChIP6.

**Figure 4.** Biz1-mediated down-regulation of *clb1* induces cell cycle arrest.

**(A)** Expression of *clb1* under a heterologous promoter avoids the down-regulation mediated by high levels Biz1. UMN53 (FB1*biz1<sup>crg1</sup>*) and UMN56 (FB1*clb1<sup>nar1</sup> biz1<sup>crg1</sup>*) cells growing in MM-NO<sub>3</sub> with glucose as carbon source, conditions in which *clb1<sup>nar1</sup>* is expressed but *biz1<sup>crg1</sup>* is repressed, were transferred to arabinose-containing MM-NO<sub>3</sub>, to allow the expression of *biz1<sup>crg1</sup>*, and samples were taken at the indicated times (in hours). RNA was isolated and submitted to RNA gel blot analysis as above, using either *biz1* or *clb1* probes, as indicated in left margin. A probe for the 18S rRNA was used as loading control.

**(B)** Expression of *clb1* under a heterologous promoter avoids the cell cycle arrest mediated by high levels Biz1. Morphology of UMN53 (FB1*biz1<sup>crg1</sup>*) and UMN56 (FB1*clb1<sup>nar1</sup> biz1<sup>crg1</sup>*) cells grown for 10 hours in MM-NO<sub>3</sub> and arabinose as carbon source. Observe the arrested phenotype of UMN53 cells while UMN56 cells showed a wild-type budding pattern. Bar, 20  $\mu$ m.

**(C)** FACS analysis of UMN53 (FB1*biz1<sup>crg1</sup>*) and UMN56 (FB1*clb1<sup>nar1</sup> biz1<sup>crg1</sup>*) cells growing in MM-NO<sub>3</sub> with arabinose as carbon source to assess DNA content in inducing conditions. Samples were taken at 0,2,4, 6, 8 and 10 hours after transfer to inducing conditions. Cells expressing *biz1* arrest their growth at G2 and thereby accumulate with a 2C DNA content, however in cells carrying the *clb1<sup>nar1</sup>* allele, cells do not accumulate in G2 phase. The shift to DNA content higher than 2C observed in UMN53 cells was due to mitochondrial DNA staining.

**Figure 5.** Phenotype of *U. maydis*  $\Delta$ *biz1* strains in axenic culture.

**(A)** Morphology of wild-type (FB1) and FB1 $\Delta$ *biz1* cells (UMN40) cells growing in nutrient-rich medium YPD. Bar 20  $\mu$ m.

**(B)** Flow cytometry analysis of the DNA content of a cell population of wild-type (FB1) and FB1 $\Delta$ *biz1* cells (UMN40) strains growing in different media (YPD, 1% glucose yeast peptone extract; CMD, 1% glucose complete medium; MMD, 1% glucose minimal medium). In different media, the 1C versus 2C DNA content changes similarly in both strains.

**(C)** Mating assays of *biz1* deletion strains. Strains indicated were spotted alone or in combinations on CM-charcoal plates and incubated at 24°C for 48 h. The appearance of white filaments indicates formation of infective hyphae.

**(D)** Quantitative analysis of nuclei distribution in wild-type and mutant infective hyphae formed by a cross of the wild-type strains FB1 and FB2 or the  $\Delta$ *biz1* mutant strains UMN40 (FB1 $\Delta$ *biz1*) and UMN41 (FB2 $\Delta$ *biz1*) after 24 h on charcoal-containing agar plates.

**(E)** Wild-type and mutant infective hyphae stained with 4',6-diamidino-2-phenylindole (DAPI) visualizing the nuclei content. Both wild-type and mutant hyphae have the same appearance, although the mutant cross resulted in filaments with an increased frequency of multiple nuclei. Arrows point to multiple nuclei in the mutant hyphae. Bar 10  $\mu$ m.

**Figure 6.** Biz1 is required for plant infection

**(A)** Filament formation of the solopathogenic strain SG200 (*a1mfa2bE1bW2*) and its derivative SG200 $\Delta$ *biz1*. Strains indicated were spotted on CM-charcoal plates and incubated at 24°C for 48 h. The white colony morphology indicates the formation of filaments.

**(B)** Influence of *biz1* deletion on pathogenicity. Maize seedlings were inoculated either with SG200 or SG200 $\Delta$ *biz1*. Six days after infection, tumors were formed on plants infected with SG200, while in infection with the mutant strain no symptoms were observed. Arrows point to the injection punctures. For a quantitative analysis, see Table 1.

**(C)** Infection of young maize plants with SG200 or SG200 $\Delta$ *biz1* results in a network of hyphae (upper row) and the production of appressoria (bottom row) that can be detected on the plant surface after 1 day by Calcofluor staining of the fungal cell wall. Bar, 100  $\mu$ m.

**(D)** Expression of yellow- and cyan-shifted derivatives of GFP (YFP and CFP) allows the identification of SG200 and SG200 $\Delta$ *biz1* strains in the same infection. Upper image shows two hyphae with appressoria (calcofluor staining). One of the appressoria is formed by SG200::CFP (fluorescence in CFP channel, middle image), the second by the SG200 $\Delta$ *biz1*::YFP mutant (fluorescence in YFP channel, bottom image).

**(E)** SG200 $\Delta$ *biz1* hyphae are impaired in appressorium formation. Equal numbers of SG200 and SG200 $\Delta$ *biz1* cells tagged with either YFP or CFP were inoculated in young maize seedlings. After one day, appressoria were scored with respect to specific CFP and YFP fluorescence. A decrease in the frequency of appressorium formation was observed in SG200 $\Delta$ *biz1*, regardless of the fluorescence marker used for tagging.

**Figure 7.**  $\Delta$ *biz1* cells arrest growth after plant penetration.

**(A)** Left: Series of Z-axis projections showing the infection of a SG200 $\Delta$ *biz1* filament. Right: Infection with SG200. Plants were infected with SG200 and

SG200 $\Delta$ *biz1*, respectively, and after two days, fungal material was visualized by staining with chlorazol black E. In SG200 $\Delta$ *biz1*, the appressorium (asterisk) and a short hyphae (arrow) that has penetrated the plant cuticle is visible. In SG200, massive proliferation of hyphae can be observed. Bar, 15  $\mu$ m.

**(B)** Series of Z-axis projections showing a top view of the infection of FB1 $\Delta$ *biz1*xFB2 $\Delta$ *biz1* hyphae that grows through the stomatal opening. Note that even at 7 days after infection, the  $\Delta$ *biz1* hypha (arrow) fails to invade the host tissue and remains in the stomatal cavity. The range of Z-axis projections (as distance in micrometers) are indicated on top-left in each microphotography. On the right, a wild type hypha (arrow) penetrating through stomata is show. Note that the wild-type hypha is able to progress through the plant tissue. Bar, 25  $\mu$ m.

**Figure 8.** The expression of *biz1* depends on *b* locus

**(A)** Northern analysis of *biz1* in different genetic backgrounds. Haploid cells (FB1 and FB2), a mixture of FB1 and FB2, diploid (FBD11) and the solopathogenic strain SG200 were grown for 36 hours on charcoal-containing plates and total RNA extracted. 10  $\mu$ g of total RNA was loaded per lane. The same filter was hybridized in succession with probes for *biz1* and 18s rRNA as loading control.

**(B)** *biz1* expression is *a*-independent but *b*-dependent. In conditions of *a* locus activation without the presence of compatible *b* loci, such as the diploid FBD12-3 (*a1 a2 b1 b1*) or the presence of an active allele of the pheromone-induced MAPKK Fuz7 in a haploid cell (FB1FuzDD) nearly undetectable expression of *biz1* was apparent. In contrast, conditions that produced an active bE/bW

heterodimer such as the AB33 strain growing resulted in high level of *biz1* expression. AB34 is a control strain carrying non-compatible *bE* and *bW* alleles. FBD12-3 cells were grown for 24 hours in charcoal-containing plates; FB1 Fuz7DD cells were grown in arabinose-containing liquid complete medium for 8 hours; AB33 and AB34 were grown for 12 hours in nitrate-containing liquid minimal medium. In all cases 10 µg of total RNA was loaded per lane. The same filter was hybridized in succession with probes for *biz1* and 18s rRNA as loading control.

**(C)** Expression of *biz1* in planta. Total RNA was extracted from plants infected with SG200 solopathogenic *U. maydis* cells at the indicated points. As control of expression out of the plant, RNA was extracted from SG200 growing in charcoal-containing plates.

**Figure 9.** High levels of *clb1* expression interferes with filament formation

**(A)** Reprogramming *clb1* expression after induction of the pathogenic program. *clb1* was placed under the control of the *dik6* promoter and ectopically integrated into the solopathogenic strain SG200 (*a1mfa2bE1/bW2*) to produce the UMN69 strain. The *dik6* promoter is induced in response to the active *bE1/bW2* heterodimer present in SG200. The expression of *bE1/bW2* in SG200 is high on charcoal-containing complete medium Ch-CMD, while on YPD plates only low *bE1/bW2* levels are observed. As a consequence, *dik6p:clb1* is highly expressed in (UMN69) on Ch-CMD. We also included SG200Δ*biz1* as control. Total RNA (10 µg) extracted from SG200 and UMN69 (SG200P<sub>*dik6*</sub>:*clb1*) cells was used for Northern analysis using *clb1*, *clb2* and 18S rRNA specific probes.

**(B)** *clb1*-reprogrammed SG200 cells are impaired in filament formation. SG200 and UMN69 (SG200P<sub>*dik6*</sub>:*clb1*) cells were spread in charcoal-containing complete medium (CMD-Ch) plates, and after 48 h. After 48 h, the SG200P<sub>*dik6*</sub>:*clb1* colonies displayed significantly less filament formation than SG200.

**(C)** Analysis of SG200P<sub>*dik6*</sub>:*clb1* hyphae from CMD-Ch medium. Cells were spotted on charcoal-containing CMD-Ch plates, and cells were recovered from the surface after 24 h. Observe the presence of cells with aberrant morphology, containing more than one nuclei in strain SG200P<sub>*dik6*</sub>:*clb1*. Bar, 20  $\mu$ m

**(D)** Appressorium formation is associated with cell-cycle arrested cells. Corn plants were infected with SG200 and SG200P<sub>*dik6*</sub>:*clb1*, respectively. 1 day after infection, appressorium formation was visualized by staining with wheat germ agglutinin and nuclear content was visualized by DAPI. Number of appressoria and number of nuclei per appressorium were counted. In SG200P<sub>*dik6*</sub>:*clb1*, we never observed appressoria with more than one nucleus.

**(E)** Examples of appressorium containing a single nucleus in SG200 and SG200P<sub>*dik6*</sub>:*clb1*, cells. WGA: wheat agglutinin staining (arrow indicates the appressorium); DAPI staining marks nucleus (asterisk indicates the nucleus); Bar, 100 $\mu$ m.

## REFERENCES

**Altschul, S.F., Gish, W., Miller, W., Myers, E.W., and Lipman, D.J. (1990)** Basic local alignment search tool. *J. Mol. Biol.* **215**, 403-410.

**Banuett, F., and Herskowitz, I.** (1989). Different *a* alleles are necessary for maintenance of filamentous growth but not for meiosis. *Proc. Natl. Acad. Sci. USA* **86**, 5878-5882.

**Banuett, F., and Herskowitz, I.** (1996). Discrete developmental stages during teliospore formation in the corn smut fungus, *Ustilago maydis*. *Development* **122**, 2965-2976.

**Banuett, F., and Herskowitz, I.** (2002). Bud morphogenesis and the actin and microtubule cytoskeletons during budding in the corn smut fungus, *Ustilago maydis*. *Fungal Genet. Biol.* **37**, 149-170.

**Basse, C.W., Kolb, S., and Kahmann, R.** (2002). A maize-specifically expressed gene cluster in *Ustilago maydis*. *Mol. Microbiol.* **43**, 75-93.

**Basse, C.W., and Steinberg, G.** (2004). *Ustilago maydis*, model system for analysis of the molecular basis of fungal pathogenicity. *Mol. Plant Pathol.* **5**, 83-92.

**Bechinger, C., Giebel, K.F., Schnell, M., Leiderer, P., Deising, H.B., and Bastmeyer, M.** (1999). Optical measurement of invasive forces exerted by appressoria of a plant pathogenic fungus. *Science* **285**, 1896-1899.

**Bölker, M., Genin, S., Lehmler, C., and Kahmann, R.** (1995). Genetic regulation of mating and dimorphism in *Ustilago maydis*. *Can. J. Bot.* **73**, S320-S325.

**Bottin, A., Kämper, J. and Kahmann, R.** (1996). Isolation of a carbon source-regulated gene from *Ustilago maydis*. *Mol. Gen. Genet.* **25**, 342-352.

**Brachmann, A., Weinzierl, G., Kämper, J. and Kahmann, R.** (2001). Identification of genes in the bW/bE regulatory cascade in *Ustilago maydis*. *Mol. Microbiol.* **42**, 1047-1063.



**Brachmann, A., Schirawski, J., Müller, P., and Kahmann, R.** (2003). An unusual MAP kinase is required for efficient penetration of the plant surface by *Ustilago maydis*. *EMBO J.* **9**, 2199-2210.

**Brachmann, A., König, J., Julius, C., and Feldbrügge, M.** (2004). A reverse genetic approach for generating gene replacement mutants in *Ustilago maydis*. *Mol. Genet. Genomics* **272**, 216-226.

**Caracuel, Z., Roncero, M.I., Espeso, E.A., Gonzalez-Verdejo, C.I., García-Maceira, F.I., and Di Pietro, A.** (2003). The pH signaling transcription factor PacC controls virulence in the plant pathogen *Fusarium oxysporum*. *Mol. Microbiol.* **48**, 765-779.

**Castillo-Lluva, S., García-Muse, T. and Pérez-Martín, J.** (2004). A member of the Fizzy-related family of APC activators is required at different stages of plant infection by *Ustilago maydis*. *J. Cell. Sci.* **117**, 4143-4156.

**Castillo-Lluva, S., and Pérez-Martín, J.** (2005). The induction of the mating program in the phytopathogen *Ustilago maydis* is controlled by a G1 cyclin. *Plant Cell* **17**, 3544-3560.

**Day, P.R., and Anagnostakis, S.L.** (1971). Corn smut dikaryon in culture. *Nat. New Biol.* **231**, 19-20.

**Dean, R.A.** (1997). Signal pathways and appressorium morphogenesis. *Ann. Rev. Phytopathol.* **35**, 211-234.

**Deising, H.B., Werner, S., and Wernitz, M.** (2000). The role of fungal appressoria in plant infection. *Microbes and Infection* **2**, 1631-1641.

**Emmett, R.W., and Parbery, D.G.** (1975). Appressoria. *Annu. Rev. Phytopathol.* **13**, 147-167.

**Escher, D., Bodmer-Glavas, M., Barberis, A., and Schaffner, W.** (2000). Conservation of Glutamine-rich transactivation function between yeast and humans. *Mol. Cell. Biol.* **20**, 2774-2782.

**García-Muse, T., Steinberg, G. and Pérez-Martín, J.** (2003). Pheromone-induced G2 arrest in the phytopathogenic fungus *Ustilago maydis*. *Eukaryotic Cell* **2**, 494-500.

**García-Muse, T., Steinberg, G. and Pérez-Martín, J.** (2004). Characterization of B-type cyclins in the smut fungus *Ustilago maydis*: roles in morphogenesis and pathogenicity. *J. Cell Sci.* **117**, 487-506.

**Garrido, E., and Pérez-Martín, J.** (2003). The *crk1* gene encodes an Ime2-related protein that is required for morphogenesis in the plant pathogen *Ustilago maydis*. *Mol. Microbiol* **47**, 729-743.

**Gillissen, B., Bergemann, J., Sandmann, C., Schrör, B., Bölker, M. and Kahmann, R.** (1992). A two-component regulatory system for self/non-self recognition in *Ustilago maydis*. *Cell* **68**, 647-657.

**Gold, R.E., and Mendgen, K.** (1991). Rust basidiospore germlings and disease initiation. In *Initiation in Plants and Animals*, G.T.Cole and H.C. Hoch, eds (New York: Plenum Press), pp. 67-99.

**Hecht, A., Strahl-Bolsinger, S., and Grunstein, M.** (1999). Mapping DNA interaction sites of chromosomal proteins. Crosslinking studies in yeast. *Methods Mol. Biol.* **119**, 469-479.

**Holliday, R.** (1974). In *Handbook of Genetics*, (ed. R. C. King) pp. 575-595, Plenum Press, New York, USA .

**Jacobs, G.H.** (1992). Determination of the base recognition positions of zinc fingers from sequence analysis. *EMBO J.* **11**, 4507-4517.

**Kahmann, R., and Kämper, J.** (2004). *Ustilago maydis*: how its biology relates to pathogenic development. *New Phytol.* **164**, 31-42.

**Kämper, J.** (2004). A PCR-based system for highly efficient generation of gene replacement mutants in *Ustilago maydis*. *Mol. Genet. Genomics* **271**, 103-110.

**Loubradou, G., Brachmann, A., Feldbrügge, M., and Kahmann, R.** (2001). A homologue of the transcriptional repressor Ssn6 antagonizes cAMP signaling in *Ustilago maydis*. *Mol. Microbiol.* **40**, 719-730.

**Matthews, J.M., and Sunde, M.** (2002). Zinc fingers: folds for many occasions. *IUBMB Life* **54**, 351-355.

**Mendgen, K., Hahn, M., and Deising, H.** (1996). Morphogenesis and mechanisms of penetration in plant pathogenic fungi. *Annu. Rev. Phytopathol.* **34**, 367-386.

**Müller, P., Weinzierl, G., Brachmann, A., Feldbrügge, M., and Kahmann, R.** (2003). Mating and pathogenic development of the smut fungus *Ustilago maydis* are regulated by one mitogen-activated protein kinase cascade. *Eukaryotic Cell* **2**, 1187-1199.

**Nakai, K., and Horton, P.** (1999). PSORT: a program for detecting the sorting signals of proteins and predicting their subcellular localization. *Trends Biochem. Sci.* **24**, 34-35.

**Nathues, E., Joshi, S., Tenberge, K.B., von der Driesch, Oeser, B., Bummer, N., Mihlan, M., and Tudzynski, P.** (2004). CPTF1, a CREB-like transcription factor, is involved in the oxidative stress response in the phytopathogen *Claviceps purpurea* and modulates ROS level in its host *Secale cereale*. *Mol. Plant Microbe Interact.* **17**, 383-393.

**Paillard, G., Deremble, C., and Lavery, R.** (2004). Looking into DNA recognition: zinc finger binding specificity. *Nucleic Acid Res.* **32**, 6673-6682.

**Park, G., Xue, C., Zheng, L., Lan, S., and Xu, J.R.** (2002). MST12 regulates infectious growth but not appressoria formation in the rice blast fungus *Magnaporthe grisea*. *Mol. Plant Microbe Interact.* **15**, 183-192.

**Pedley, K.F., and Walton, J.D.** (2001). Regulation of cyclic peptide biosynthesis in a plant pathogenic fungus by a novel transcription factor. *Proc. Natl. Acad. Sci. USA* **98**, 14174-14179.

**Romeis, T., Brachmann, A., Kahmann, R., and Kämper, J.** (2000). Identification of a target gene for the be-bW homeodomain protein complex in *Ustilago maydis*. *Mol. Microbiol.* **37**, 54-66.

**Sgarlata, C. and Pérez-Martín, J.** (2005a). Inhibitory phosphorylation of a mitotic cyclin-dependent kinase regulates the morphogenesis, cell size and virulence of the smut fungus *Ustilago maydis*. *J. Cell. Sci.* **15**, 3607-3622.

**Sgarlata, C. and Pérez-Martín, J.** (2005b). The Cdc25 phosphatase is essential for the G2/M phase transition in the basidiomycete *Ustilago maydis*. *Mol. Microbiol.* **58**, 1482-1496.

**Sherman, F., Fink, G.R. and Hicks, J.B.** (1986). Laboratory course manual for methods in yeast genetics (Cold Spring Harbor, NY: Cold Spring Harbor Laboratory Press).

**Snetselaar, K.M., and Mims, C.W.** (1992). Sporidial fusion and infection of maize seedlings by the smut fungus *Ustilago maydis*. *Mycologia*, **84**, 193-203.

**Snetselaar, K.M., and Mims, C.W.** (1993). Infection of maize stigmas by *Ustilago maydis*: light and electron microscopy. *Phytopathology* **83**, 843-850.

**Snetselaar, K.M., Bölker, M., and Kahmann, R.** (1996). *Ustilago maydis* mating hyphae orient their growth toward pheromone sources. *Fungal Genet. Biol.* **20**, 299-312.

**Snetselaar, K.M., Carfioli, M.A., and Cordisco, K.M.** (2001). Pollination can protect maize ovaries from infection by *Ustilago maydis*, the corn smut fungus. *Can. J. Bot.* **79**, 1390-1399.

**Spellig, T., Bölker, M., Iottspeich, F., Frank, R.W., and Kahmann, R.** (1994). Pheromones trigger filamentous growth in *Ustilago maydis*. *EMBO J.* **13**, 1620-1627.

**Steinberg, G., Schliwa, M., Lehmler, C., Bölker, M., Kahmann, R., and McIntosh, J.R.** (1998). Kinesin from the plant pathogenic fungus *Ustilago maydis* is involved in vacuole formation and cytoplasmic migration. *J. Cell Sci.* **111**, 2235-2246.

**Steinberg, G., Wedlich-Söldner, R., Brill, M., and Schulz, I.** (2001). Microtubules in the fungal pathogen *Ustilago maydis* are highly dynamic and determine cell polarity. *J. Cell Sci.* **114**, 609-622.

**Suzuki, M., Gerstein, M., and Yagi, N.** (1994). Stereochemical basis of DNA recognition by Zn fingers. *Nucleic Acid Res.* **22**, 3397-3405.

**Talbot, N.J.** (2003). On the trail of a cereal killer: Exploring the biology of *Magnaporthe grisea*. *Annu. Rev. Microbiol.* **57**, 177-202.

**Tsukuda, T., Carleton, S., Fotheringham, S. and Holloman, W.K.** (1988). Isolation and characterization of an autonomously replicating sequence from *Ustilago maydis*. *Mol. Cell. Biol.* **8**, 3703-3709.

**Veneault-Fourrey, C., Barooah, M., Egan, M., Wakley, G., and Talbot, N. J.**

(2006). Autophagic fungal cell death is necessary for infection by the rice blast fungus. *Science* **312**, 580-583.

**Weber, I., Gruber, C., and Steinberg, G.** (2003). A class V myosin required for

mating, hyphal growth and pathogenicity in the dimorphic plant pathogen *Ustilago maydis*. *Plant Cell* **15**, 2826-2842.

**Wolfe S. A., Nekludova, L., and Pabo C. O.** (1999). DNA recognition by

Cys<sub>2</sub>His<sub>2</sub> zinc finger proteins. *Annu. Rev. Biophys. Biomol. Struct.* **3**, 183-212.

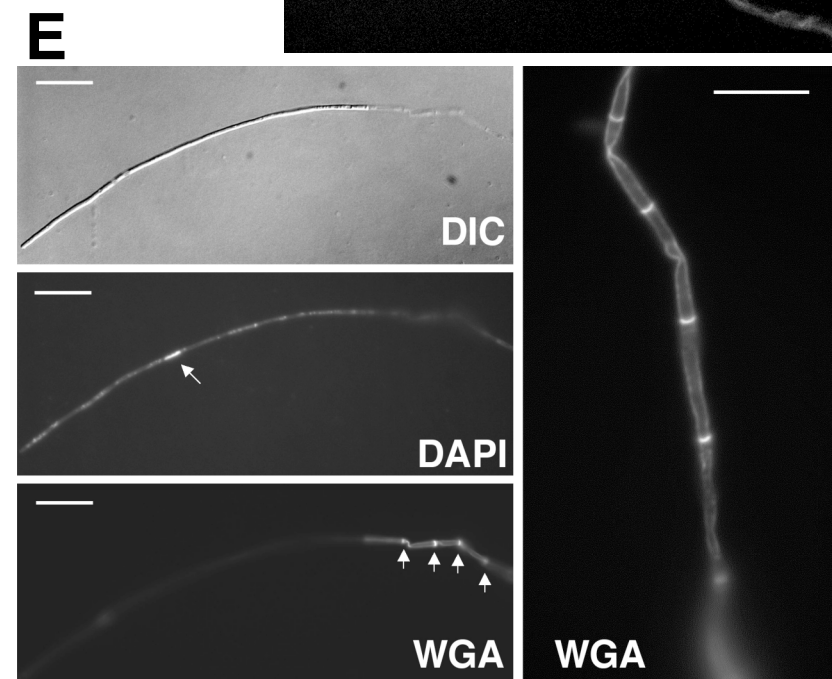
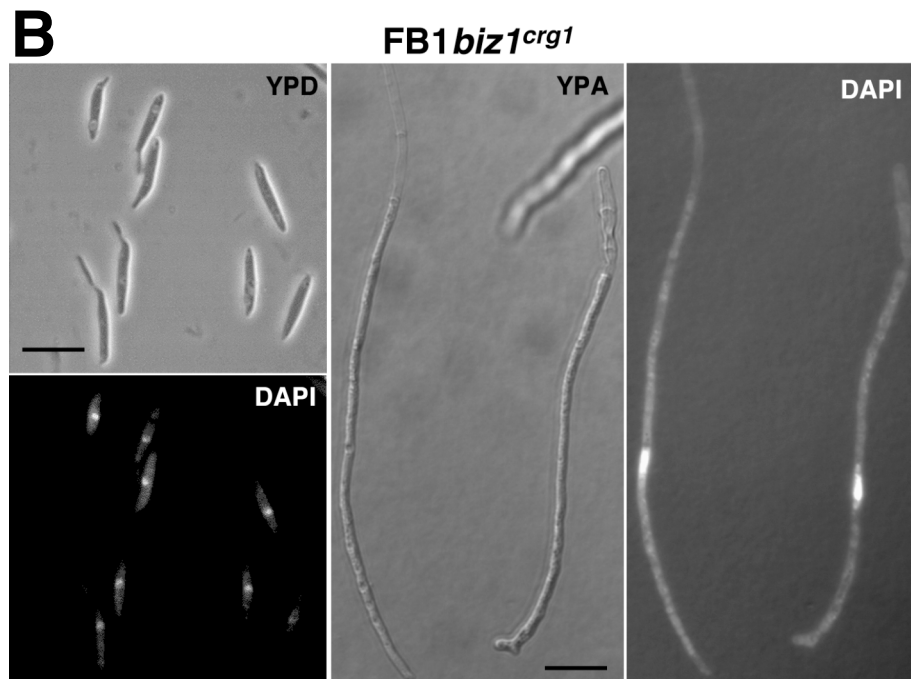
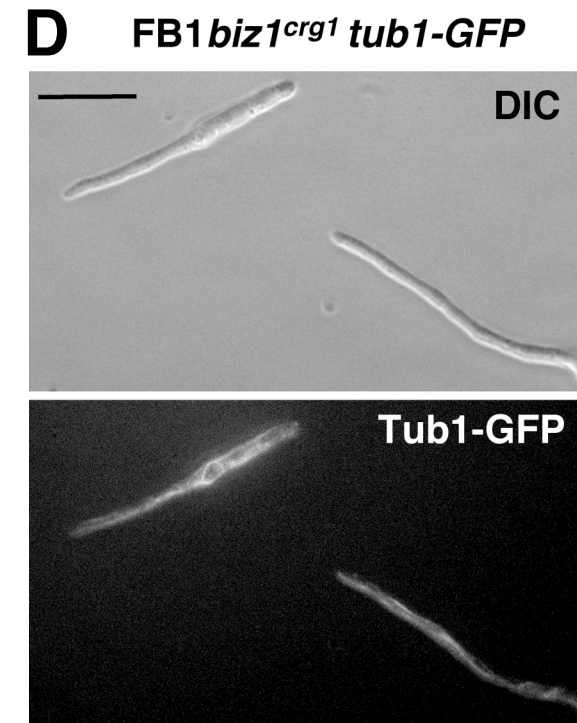
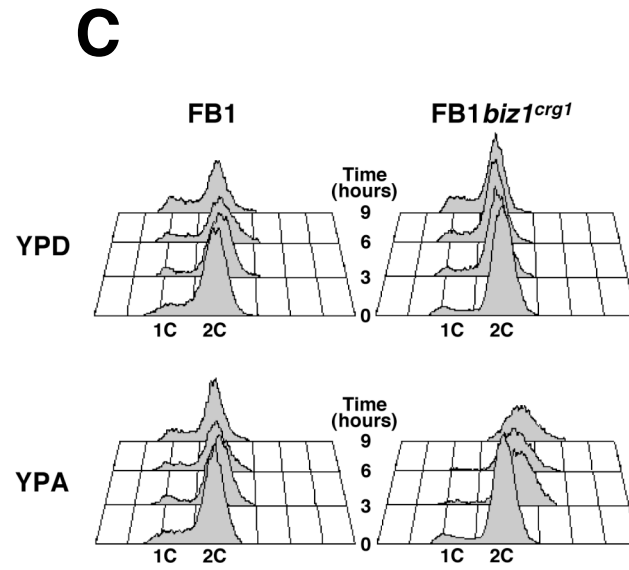
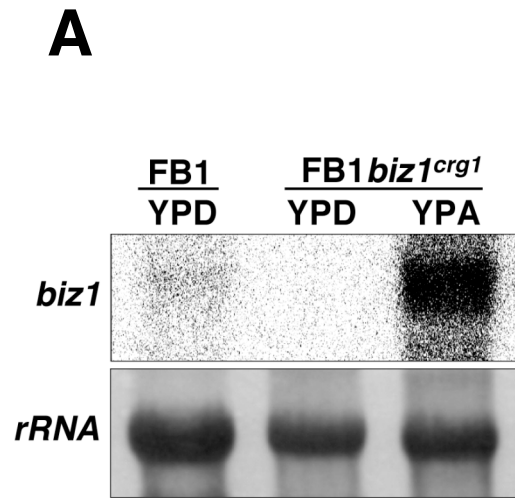
**Table 1.** Pathogenicity assays

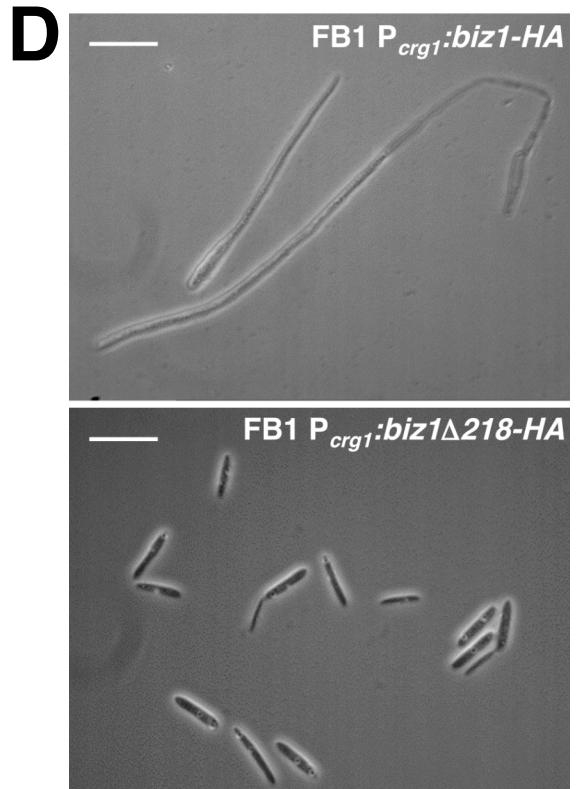
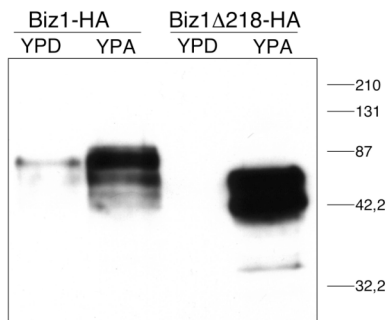
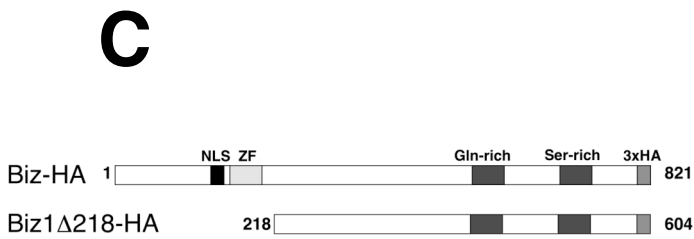
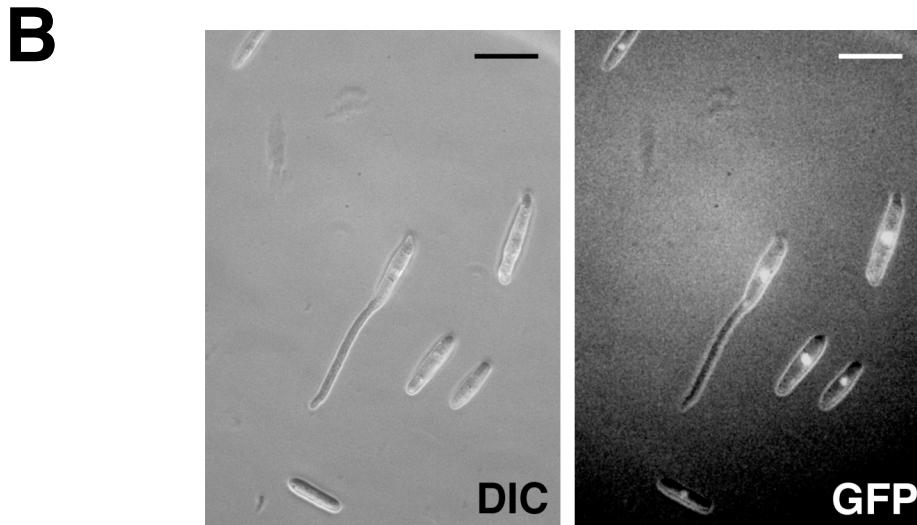
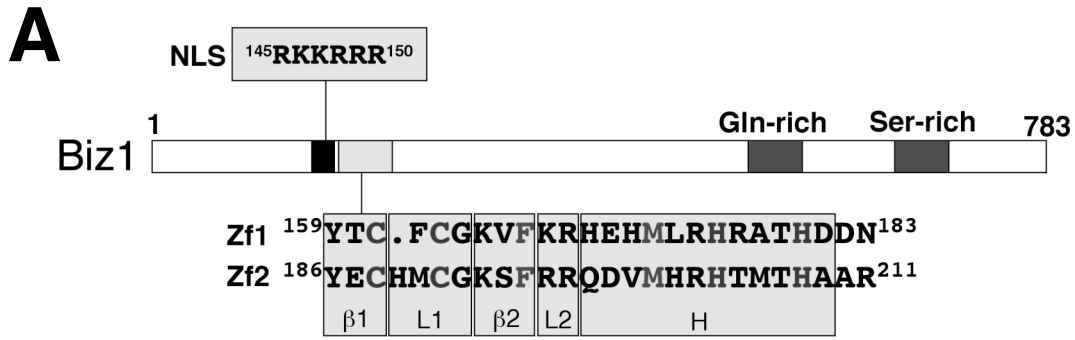
Inoculum	Genotype	Tumor formation	
		Total	Percentage
FB1 x FB2	<i>a1 b1 x a2 b2</i>	62/69	89
UMN40 x UMN41	<i>a1 b1 Δbiz1 x a2 b2 Δbiz1</i>	0/74	0
SG200	<i>a1mfa2 bW2bE1</i>	59/70	84
SG200Δbiz1	<i>a1mfa2 bW2bE1 Δbiz1</i>	0/82	0
UMN69	<i>a1mfa2 bW2bE1 P<sub>dik6</sub>:clb1</i>	29/62	46

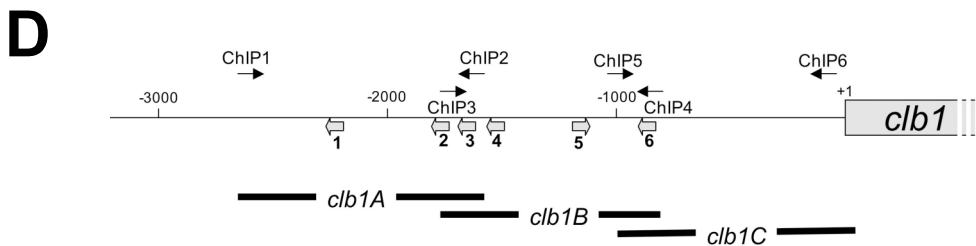
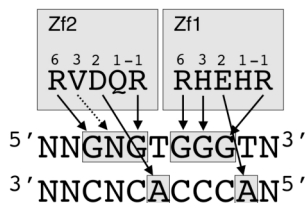
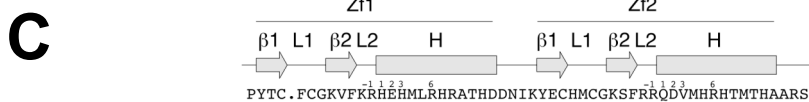
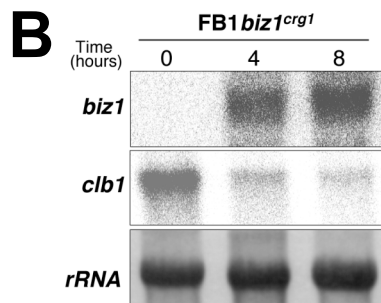
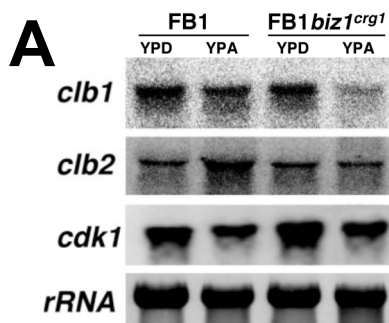
**Table 2.** *U. maydis* strains used in this study

Strain	Relevant genotype	Reference
FB1	<i>a1 b1</i>	Banuett and Herskowitz, 1989
FB2	<i>a2 b2</i>	Banuett and Herskowitz, 1989
FBD11	<i>a1a2 b1b2</i>	Banuett and Herskowitz, 1989
FBD12-3	<i>a1 a2 b1 b1</i>	Banuett and Herskowitz, 1989
SG200	<i>a1 mfa2 bW2 bE1</i>	Bölker et al., 1995
AB33	<i>a2 P<sub>nar1</sub>:bW2 P<sub>nar1</sub>:bE1</i>	Brachmann et al., 2001
AB34	<i>a2 P<sub>nar1</sub>:bW2 P<sub>nar1</sub>:bE2</i>	Brachmann et al., 2001
FB1P <sub>crg1</sub> :fuz7DD	<i>a1 b1 P<sub>crg1</sub>:fuz7<sup>DD</sup></i>	Müller et al., 2003
UMN40	<i>a1 b1 Δbiz1</i>	This work
UMN41	<i>a2 b2 Δbiz1</i>	This work
UMN45	<i>a1 b1P<sub>crg1</sub>:biz1-3HA</i>	This work
UMN47	<i>a1 b1P<sub>crg1</sub>:biz1</i>	This work
UMN52	<i>a1 b1P<sub>crg1</sub>:biz1-gfp</i>	This work
UMN53	<i>a1 b1 biz1<sup>crg1</sup></i>	This work
UMN56	<i>a1 b1 clb1<sup>nar1</sup> biz1<sup>crg1</sup></i>	This work
UMN68	<i>a1 b1 biz1<sup>crg1</sup> tub1-GFP</i>	This work
UMN69	<i>a1 mfa2 bW2 bE1 P<sub>dik6</sub>:clb1</i>	This work
UMN75	<i>a1 b1P<sub>crg1</sub>:biz1Δ218-3HA</i>	This work
SG200Δbiz1	<i>a1 mfa2 bW2 bE1 Δbiz1</i>	This work
SG200CFP	<i>a1 mfa2 bW2 bE1 P<sub>OMA</sub>:CFP</i>	This work
SG200YFP	<i>a1 mfa2 bW2 bE1 P<sub>OMA</sub>:YFP</i>	This work
SG200Δbiz1CFP	<i>a1 mfa2 bW2 bE1 Δbiz1 P<sub>OMA</sub>:CFP</i>	This work
SG200Δbiz1YFP	<i>a1 mfa2 bW2 bE1 Δbiz1 P<sub>OMA</sub>:YFP</i>	This work

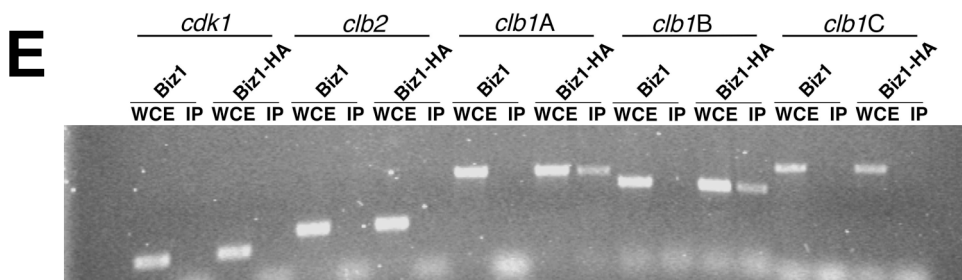




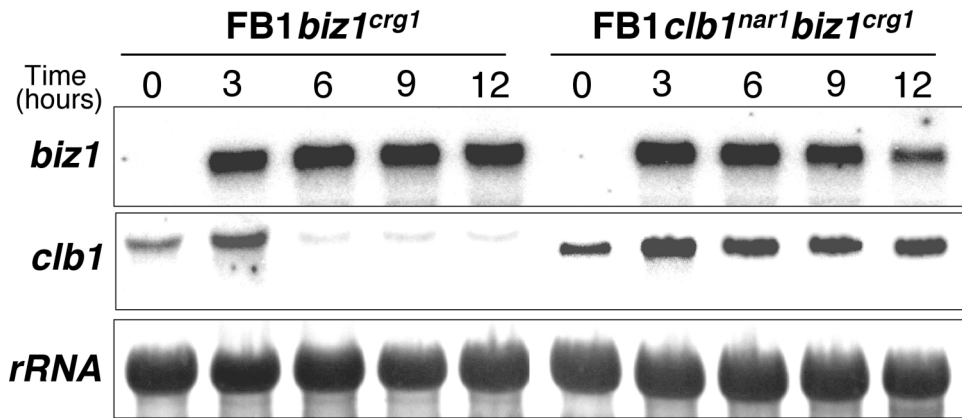




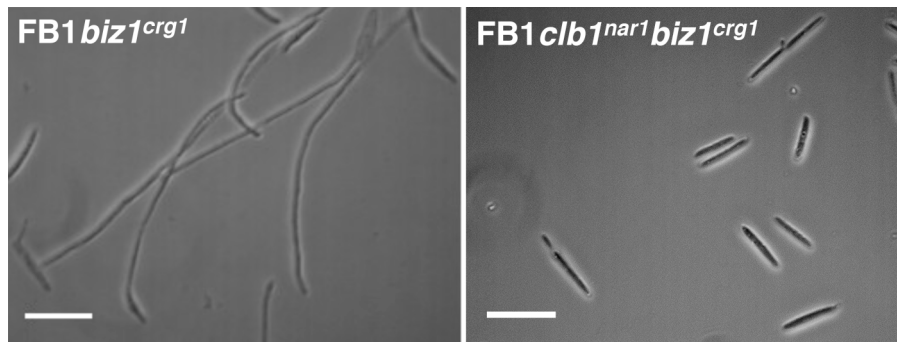
5' GNGTGGGT<sup>3'</sup> Theoretical sequence  
 5' GTGTGcGT<sup>3'</sup> Hit #1 (-2220)  
 5' GAGTGGGa<sup>3'</sup> Hit #2 (-1824)  
 5' GAGTtGGT<sup>3'</sup> Hit #3 (-1759)  
 5' GTGTGGaT<sup>3'</sup> Hit #4 (-1590)  
 5' GTGTtGGT<sup>3'</sup> Hit #5 (-1365)  
 5' GCGTtGGT<sup>3'</sup> Hit #6 (-950)



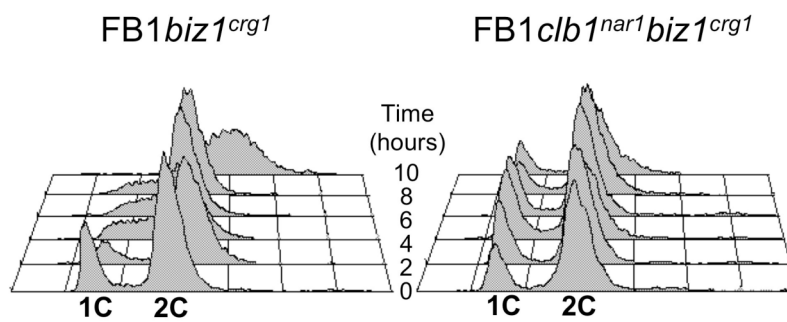
# A

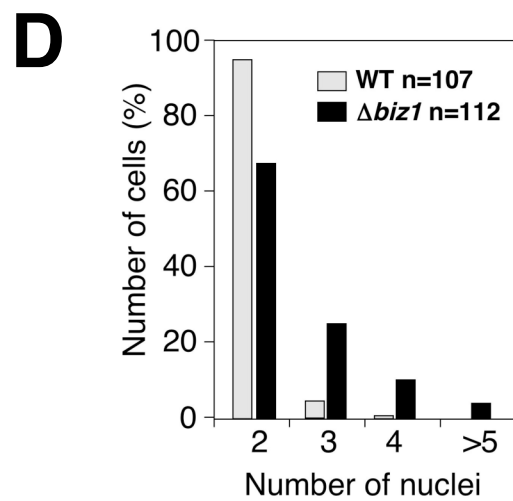
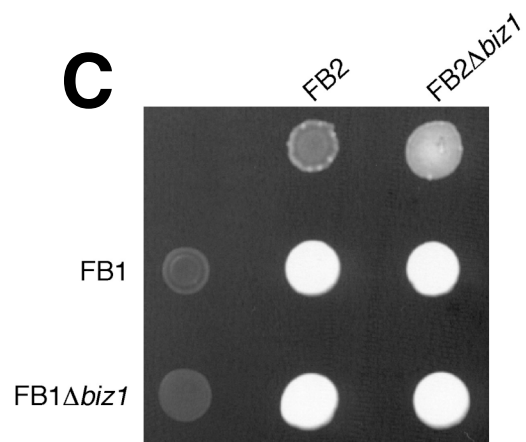
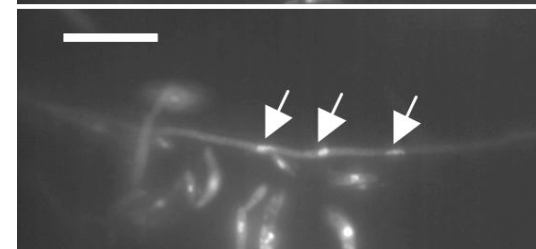
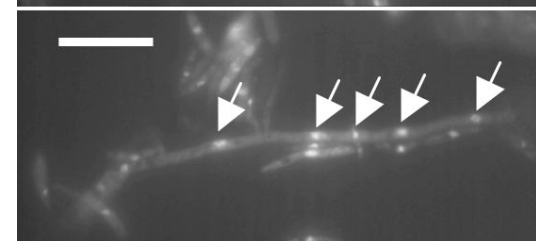
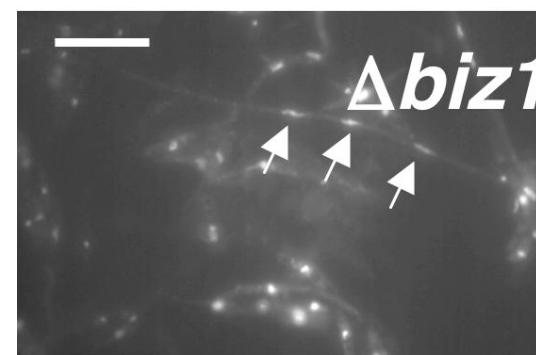
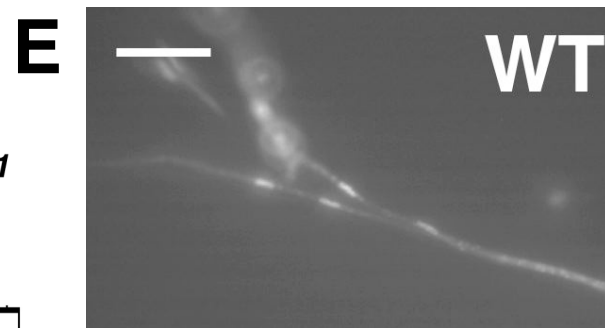
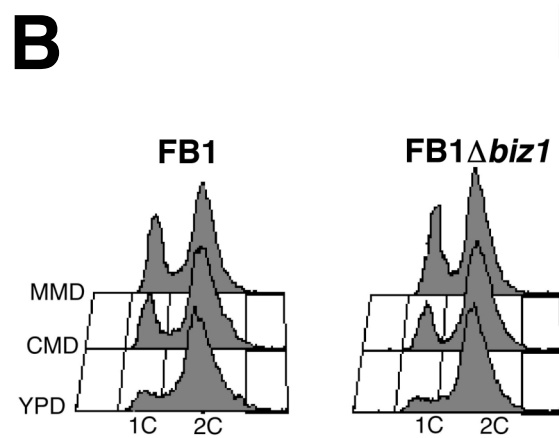
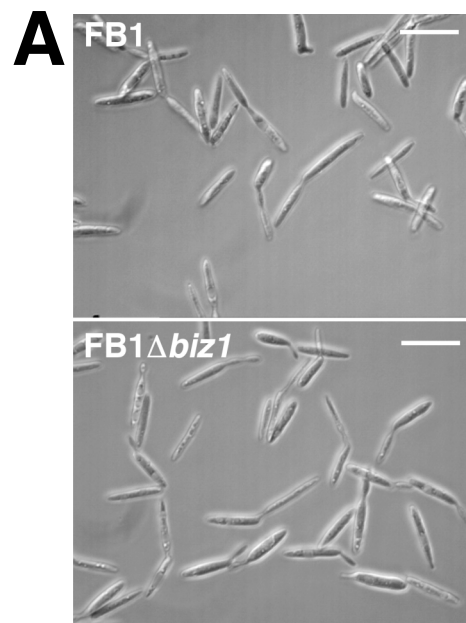


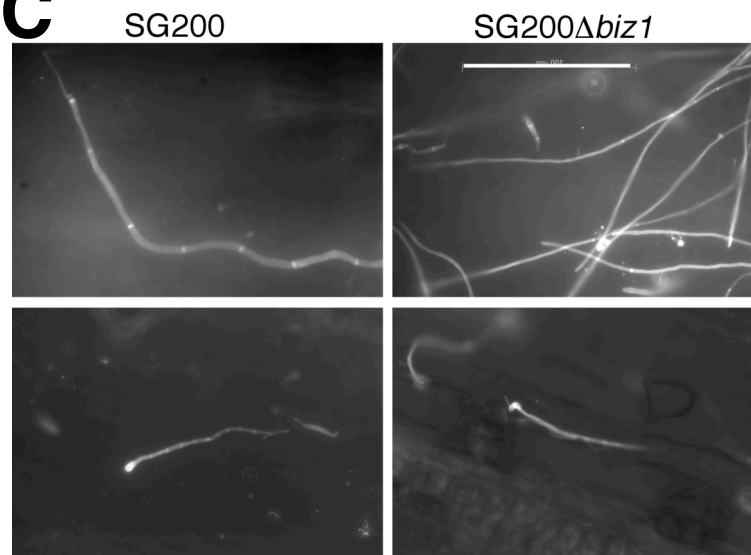
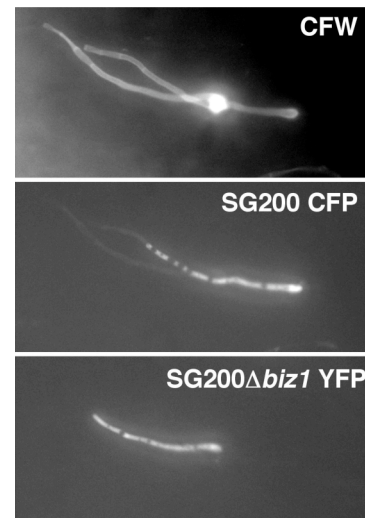
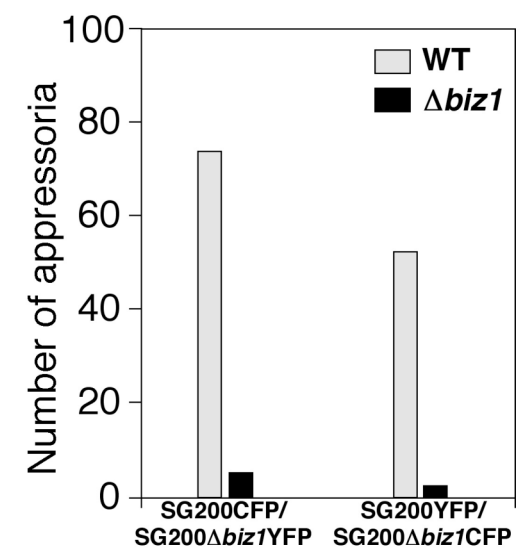
# B



# C

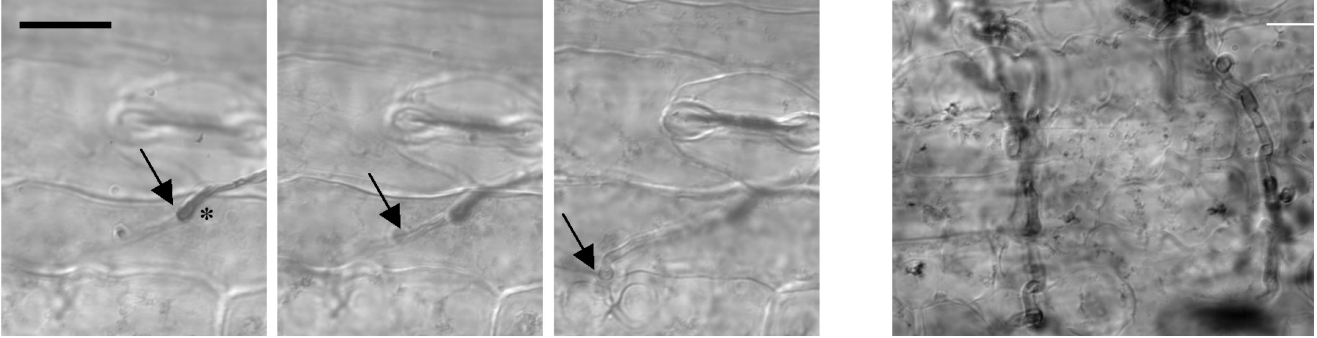




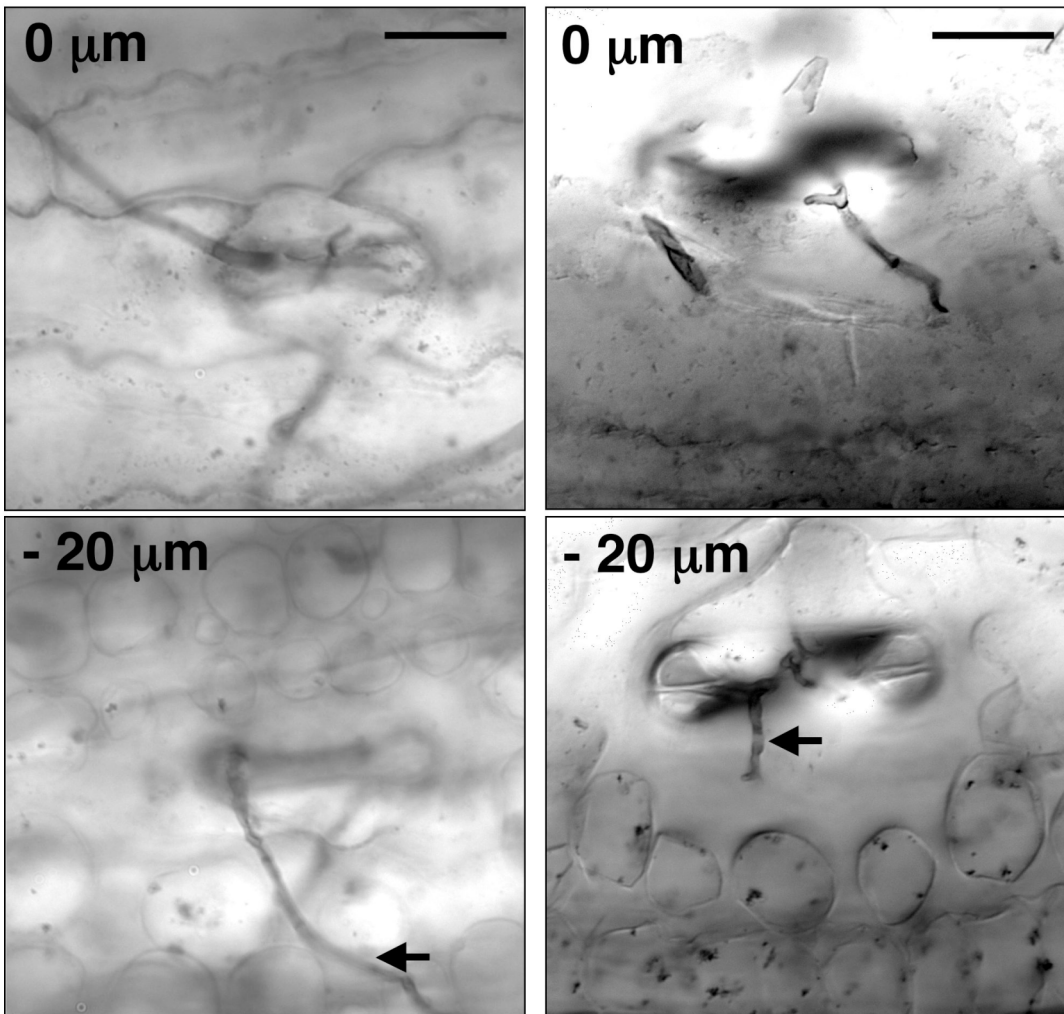
**A****B****C****D****E**

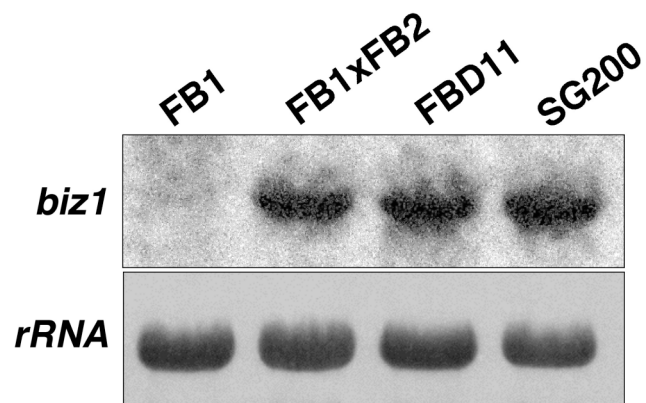
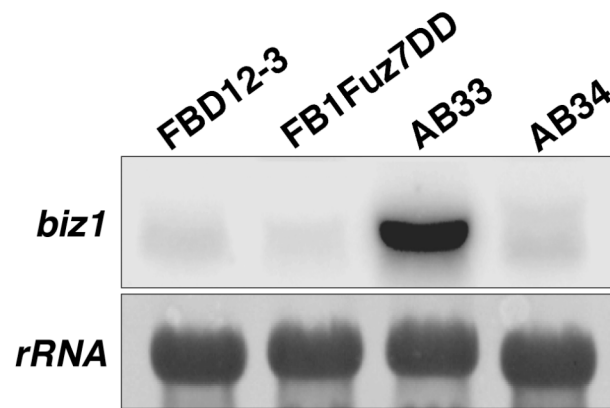
**A**SG200 $\Delta$ *biz1*

SG200

**B**

FB1xFB2

FB1 $\Delta$ *biz1* x FB2 $\Delta$ *biz1*

**A****B****C**